1

Newton, Fizeau, and Haidinger Interferometers

M. V. Mantravadi and D. Malacara

1.1. INTRODUCTION

This chapter has been updated by the second author; it includes much of the material from the previous version of the book. Newton, Fizeau, and Haidinger interferometers are among the simplest and most powerful tools available to a working optician. With very little effort, these interferometers can be set up in an optical workshop for routine testing of optical components to an accuracy of a fraction of the wavelength of light. Even though these instruments are simple in application and interpretation, the physical principles underlying them involve a certain appreciation and application of physical optics. In this chapter, we examine the various aspects of these interferometers and also consider the recent application of laser sources to them. The absolute testing of flats will also be considered in this chapter.

1.2. NEWTON INTERFEROMETER

We will take the liberty of calling any arrangement of two surfaces in contact illuminated by a monochromatic source of light a Newton interferometer. Thus, the familiar setup to obtain Newton rings in the college physical optics experiment is also a Newton interferometer; the only difference being the large air gap as one moves away from the point of contact, as seen in Figure 1.1. Because of this, it is sometimes necessary to view these Newton rings through a magnifier or even a low-power microscope. In the optical workshop, we are generally concerned that an optical flat, one being fabricated, is matching the accurate surface of another reference flat or that a curved spherical surface is matching the correspondingly opposite curved spherical master surface. Under these conditions, the air gap is seldom more than a few wavelengths of light in thickness. In the various forms of the

Optical Shop Testing, Third Edition Edited by Daniel Malacara

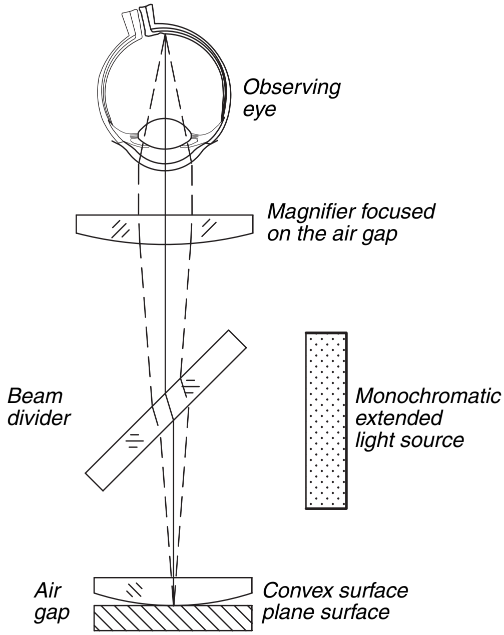

FIGURE 1.1. Illustration of the setup for Newton rings. A plano-convex lens of about 1 or 2 m in focal length is placed with its convex surface in contact with the plano surface of an optical flat and illuminated by monochromatic light.

Newton interferometer, we are mainly interested in determining the nonuniformity of this air gap thickness by observing and interpreting Newton fringes. A simple way to observe these Newton fringes is illustrated in Figure 1.2. Any light source such as a sodium vapor lamp, low-pressure mercury vapor lamp, or helium discharge lamp can be used in the setup. Under certain situations, even an ordinary tungsten lamp can serve this purpose.

Let us first see what happens when two perfect optical flats are placed one over the other with only a thin air gap between them as illustrated in Figure 1.3. The surfaces are not exactly parallel, so that the air gap is thinner on the left than on the right. Generally this separation is not zero at any place, unless the surfaces are extremely clean, and one presses very hard to get them in close contact. Hence, we may imagine that the two planes are projected backward, as shown in Figure 1.3, and they meet at a line of intersection. Let the monochromatic light of wavelength λ be incident on the optical flat combination having an angle α between them, almost normally. If the air gap is x at a given point, the two reflected rays will have an optical path difference (OPD) equal to $2x$. One of the reflected rays is reflected internally on one of the surfaces, while the other is reflected externally. We know that in dielectrics, like glass, one of these two reflected rays, and only one of them, has a phase change by 180°. In this case it is the reflected ray on the bottom surface which will have this phase change. Thus, the phase difference between the two reflected rays will produce a dark fringe when the optical path difference is an

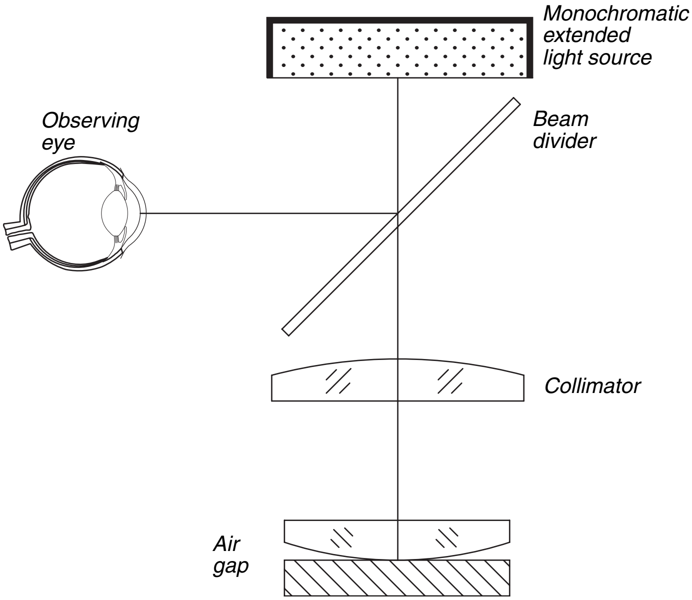

FIGURE 1.2. A simple arrangement to observe the Newton fringes in the optical workshop. With this arrangement plane and long radius spherical surfaces can be tested.

integer multiple of the wavelength. We may easily conclude that if the separation x is zero, there is a dark fringe.

Hence the dark fringes may be represented by

$$2\alpha x = n\lambda, \tag{1.1}$$

where n is an integer, and the bright fringes may be represented by

$$2\alpha x + \frac{\lambda}{2} = n\lambda. \tag{1.2}$$

Each of these equations represents a system of equally spaced straight fringes, and the distance d between two consecutive bright or dark fringes is

$$d = \frac{\lambda}{2\alpha}. \tag{1.3}$$

Thus the appearance of the fringes is as shown in Figure 1.3, when two good optical flats are put in contact with each other, forming a small air wedge, and are viewed in monochromatic light.

Now let us see what the appearance of Newton fringes is when one surface is optically flat while the other surface is not. Several situations are possible and in fact occur in actual practice. When one starts making a surface a plane, it does not turn out to be a plane on the first try; probably it becomes spherical with a long radius of curvature. It is necessary to test the surface from time to time with a reference flat to

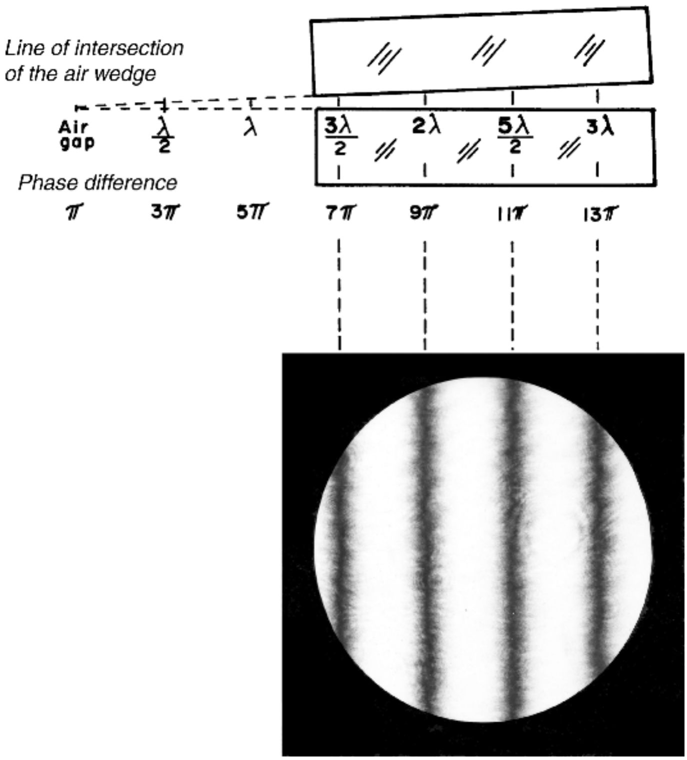

FIGURE 1.3. The principle of the formation of straight, equally spaced fringes between two optically plane surfaces when the air gap is in the form of a wedge. The fringes are parallel to the line of intersection of the two plane surfaces.

ascertain its deviation from flatness. Let us consider a spherical surface of large radius of curvature R in contact with the optical flat.

Then the sag of the surface is given by $x^2/2R$, where x is the distance measured from the center of symmetry. Hence the OPD is given by $x^2/R + \lambda/2$, and the positions of the dark fringes are expressed by

$$\frac{x^2}{R} = n\lambda. \tag{1.4}$$

Hence the distance of the nth dark fringe from the center is given by

$$x_n = \sqrt{nR\lambda}. \tag{1.5}$$

From this, it is easy to show that the distance between the $(n+1)$th and the nth fringe is given by

$$x_{n+1} - x_n = \sqrt{R\lambda}(\sqrt{n+1} - \sqrt{n}), \tag{1.6}$$

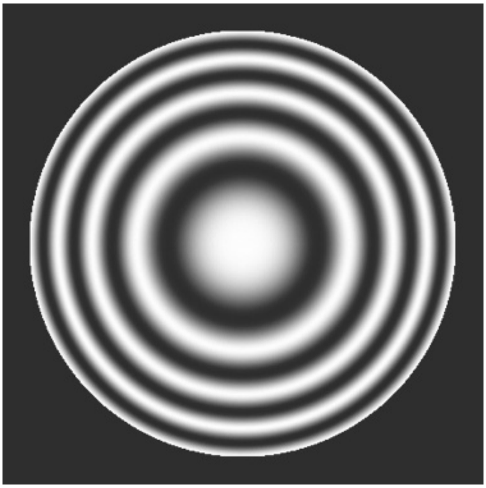

FIGURE 1.4. Appearance of the Newton fringes when a long radius of curvature is kept on a good optical flat. This situation is for a surface deviating 2λ from the plane at its maximum.

and similarly the distance between the $(n+2)$th and the $(n+1)$th fringe is given by

$$x_{n+2} - x_{n+1} = \sqrt{R\lambda}(\sqrt{n+2} - \sqrt{n+1}). \tag{1.7}$$

From Eqs. (1.6) and (1.7) we can form the ratio

$$\frac{x_{n+1} - x_n}{x_{n+2} - x_{n-1}} \approx 1 + \frac{1}{2n}. \tag{1.8}$$

Thus, it is seen that when we look at fringes with large values of n, they appear to be almost equally spaced. Hence, when we are testing for the presence of curvature in the surface, it is desirable to manipulate the plates in such a way that we see the fringes with lower order n. In Figure 1.4, the appearance of Newton fringes is shown when the maximum value of $x^2/2R$ is $2\ \lambda$. Thus, there will be four circular fringes in this situation. If the maximum value of $x^2/2R$ is $\lambda/2$, we have just one circular fringe. Thus, by observation of full circular fringes, we can detect a maximum error of $\lambda/2$ in the flatness of the surface. If the maximum error is less than $\lambda/2$, we have to adopt a different procedure. In this case, the center of the symmetry of the circular fringes is displaced sideways by suitable manipulation of the two components. Thus, we obtain fringes in the aperture of the two surfaces in contact with a larger value of n; these fringes are arcs of circles, and their separations are almost, but not exactly, equal. Let us take as examples of maximum value $x^2/2R = \lambda/4$ and $\lambda/8$. Figures 1.5 and 1.6, respectively, illustrate the appearance of the fringes in these two cases. As can be inferred, the fringes become straighter and straighter as the value of R increases.

In the optical workshop, it is also necessary to know whether the surface that is being tested is concave or convex with respect to the reference optical flat. This can

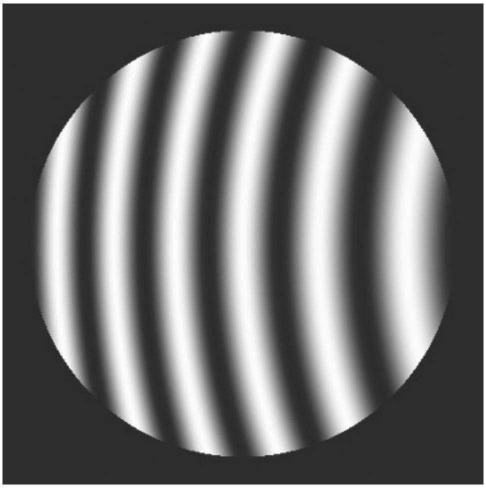

FIGURE 1.5. Appearance of the Newton fringes when a surface of long radius of curvature is kept on a good optical flat. This situation is for a surface deviating by $\lambda/4$ from the plane at its maximum. The center of symmetry of the fringes is outside the aperture of the surfaces, and hence only arcs of circles are seen.

be easily judged by several procedures. One simple method involves pressing near the edge of the top flat gently by means of a wooden stick or pencil. If the surface is convex, the center of the fringe system moves toward the point of the application of pressure. If the surface is concave, the center of the fringe system moves away from the point of the application of pressure, as shown in Figure 1.7 (a).

A second very simple method is to press near the center of the ring system on the top flat, as shown in Figure 1.7 (b). If the surface is convex, the center of the fringe is not displaced but the diameter of the circular fringes is increased.

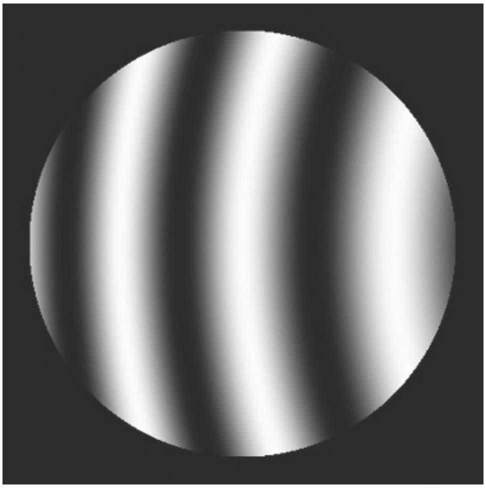

FIGURE 1.6. Same as Figure 1.5 except that the maximum error is $\lambda/8$ and some tilt is introduced.

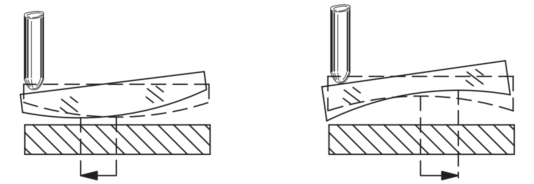

(a) Displacement of the center of rings

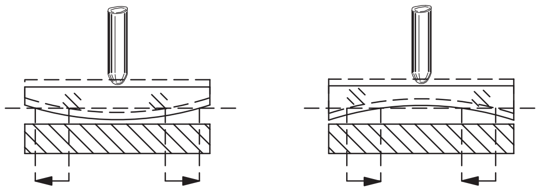

(b) Enlargement or contraction of rings

FIGURE 1.7. Two methods to determine whether the surface under test is convex or concave with respect to the surface: (a) by pressing near the edge and (b) by pressing near the center of the top plate.

Another method of deciding whether the surface is convex or concave involves the use of a source of white light. If slight pressure is applied at the center of the surfaces, the air gap at this point tends to become almost zero when the surface is convex. Hence the fringe at this point is dark, and the first bright fringe will be almost colorless or white. The next bright fringe is tinged bluish on the inside and reddish on the outside. On the contrary, if the surface is concave, the contact is not a point contact but occurs along a circle, and the air gap thickness tends to become zero along this circle. The dark fringe will be along this circle, and the sequence of colored fringes will be the same as before as one proceeds from the black fringe. This situation is illustrated in Figures 1.8 and 1.9. This procedure is not very easy to perform unless the surfaces are clean and is not generally recommended.

A fourth and simpler procedure is based on the movement of the fringe pattern as one moves the eye from a normal to an oblique viewing position. Before explaining this procedure, it is necessary to find a simple expression for the optical path difference between the two reflected rays at an air gap of thickness t and an angle of incidence θ. This is illustrated in Figure 1.10, where it can be seen that

$$\mathrm{OPD} = \frac{2t}{\cos\theta} - 2t\tan\theta\sin\theta = 2t\cos\theta. \tag{1.9}$$

Thus, the OPD at the normal of incidence, namely $2t$, is always greater than the OPD at an angle θ for the same value of air gap thickness t. Using this fact, let us see what happens when we have a convex contact between the two surfaces. The air gap increases as we go away from the point of contact. When we view the fringes obliquely, the OPD at a particular point is decreased, and consequently the fringes appear to move away from the center as we move our eye from the normal to oblique

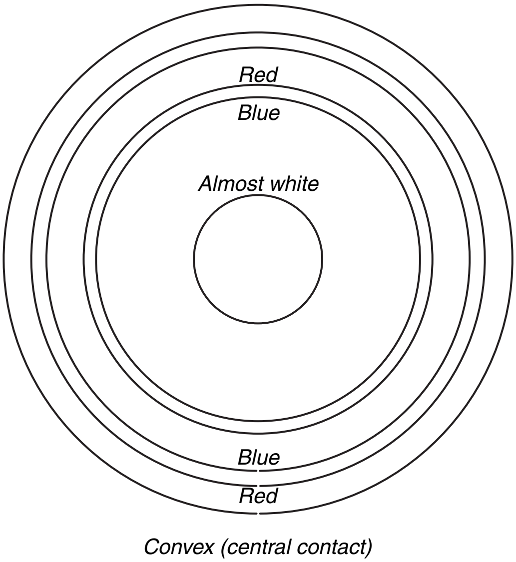

FIGURE 1.8. Convex contact and appearance of the colored fringes with white light illumination. Pressure is applied at the center.

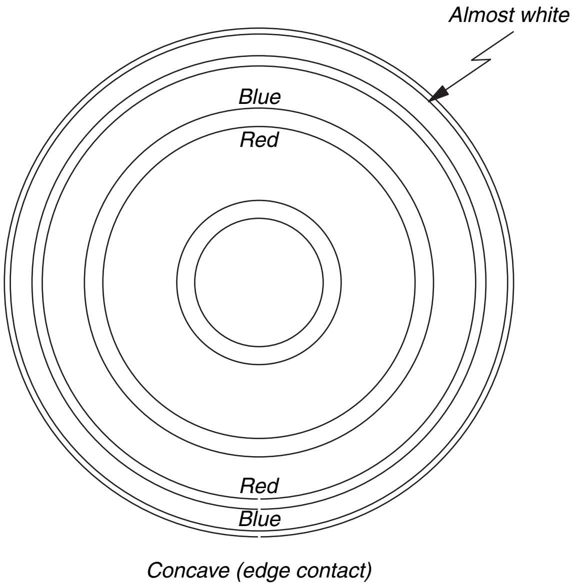

FIGURE 1.9. Convex contact and appearance of the colored fringes with white light illumination. Pressure is applied at the center.

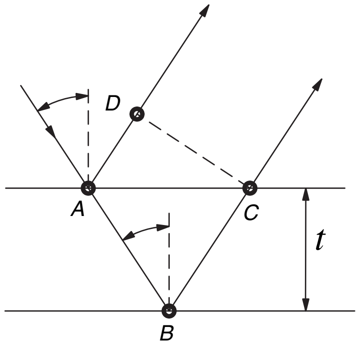

OPD = $AB ++ BC - AD = 2\,t\cos\theta$

FIGURE 1.10. Ray diagram for calculation of the optical path difference between two reflected rays from an air gap of thickness t and angle of incidence θ.

position. The reverse of this situation occurs for a concave surface in contact with a plane surface.

We may consider many other situations where the surfaces are not plane or spherical. The nature and the appearance of such fringes when viewed are given in the usual manner in Table 1.1.

We have mentioned that the reference surface is a flat surface against which a nearly plane surface that is being made is tested. By the same procedure, spherical or cylindrical surfaces having long radii of curvature can be tested. However, when such surfaces have very short radii of curvature, it is necessary to use special illumination, which will be discussed in Section 1.2 on the Fizeau interferometer.

1.2.1. Source and Observer's Pupil Size Considerations

The OPD given in Eq. (1.9) shows that this value depends on the angle of the reflected rays being observed, which for small angles θ can be approximated by

$$\text{OPD} = 2t\cos\theta \approx 2t - t\theta^2. \tag{1.10}$$

Now, in the Newton interferometer we are interested in measuring glasses where t is not constant and thus θ is not constant either. Hence, to reduce the influence of θ, as much as possible, we should have

$$t\theta^2 \leq \frac{\lambda}{k}, \tag{1.11}$$

where λ/k is the maximum allowed error due to variations in θ. Typically, to have a reasonably small error, we at least require that

$$t\theta^2 \leq \frac{\lambda}{4}. \tag{1.12}$$

TABLE 1.1. Nature of Newton fringes for different surfaces with reference to a standard flat.

		Appearance of the Newton fringes	
S. No.	Surface type	Without tilt	With tilt
1	Plane	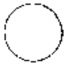	
2	Almost plane	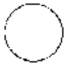	
3	Spherical		
4	Conical		
5	Cylindrical		
6	Astigmatic (curvatures of same sign)		
7	Astigmatic (curvatures of opposite sign)		
8	Highly irregular		

Thus, to ensure a small error, both t and θ should be small. Regarding the value of t, we may safely assume that the value of t should never exceed a few wavelengths in the gap. If the surfaces are clean, then flat t should not exceed about 6λ. With this maximum value of t, the maximum allowed value of θ is such that $\theta^2 \leq 1/24$ or $\theta \leq 0.2$. For example, let us set the accuracy, to which the thickness t is to be assessed, to be equal to $\lambda/20$, thus, writing Eq. (1.12) as

$$t\theta^2 \leq \frac{\lambda}{20} \text{ or } 2\theta \leq 0.2. \tag{1.13}$$

From the foregoing analysis, it can be seen that the illumination angle on the two flats in contact should never exceed 0.2 rad or 12° approximately.

The size of the light source becomes irrelevant if the angular diameter of the entrance pupil of the observer, as seen from the flats, is smaller than this value. The light source can thus be extended to any size. It is only necessary that the observation, visual or photographic, is made nearly perpendicular to the flats and from a minimum distance, such that it is roughly five times the diameter of the optical flats in contact. To obtain higher accuracy, the distance from which the observation is made has to be larger. Alternatively, a collimating lens can be used and the entrance pupil of the observing eye or camera is then placed at the focus of the collimator.

If the observing distance is not large enough, equal thickness fringes will not be observed. Instead, localized fringes will appear. These fringes are called localized because they seem to be located either above or below the air gap. The fringes are localized in the region where corresponding rays from the two virtual images of the light source intersect each other. It has been shown that this condition may be derived from the van Cittert–Zernike theorem (Wyant, 1978; Simon and Comatri, 1987; Hariharan and Steel, 1989).

1.2.2. Some Suitable Light Sources

For setting up a Newton interferometer, we require a suitable monochromatic source. Several sources are available and are convenient. One source is, of course, a sodium vapor lamp, which does not require any filter. Another source is a low-pressure mercury vapor lamp with a glass envelope to absorb the ultraviolet light. A third possible source is a helium discharge lamp in the form of a zigzag discharge tube and with a ground glass to diffuse the light. Table 1.2 gives the various wavelengths that can be

TABLE 1.2. Characteristics, such as wavelength, of various lamps suitable as light sources in Newton's interferometer.

Serial number	Lamp type	Wavelength(s) normally used (nm)	Remarks
1	Sodium vapor	589.3	The wavelength is the average of the doublet 589.0 and 589.6 nm. Warm-up time is about 10 min.
2	Low-pressure mercury vapor	546.1	Because of other wavelengths of mercury vapor present, the fringes must be viewed through the green filter, isolating the 546.1 nm line. There is no warm-up time. Tube lights without fluorescent coating can be used.
3	Low-pressure helium discharge	587.6	Because of other wavelengths of helium discharge present, a yellow filter must be used to view the fringes.There is no warm-up time.
4	Thallium vapor	535.0	Characteristics are similar to those of the sodium vapor lamp. Warm-up time is about 10 min.
5	Cadmium vapor	643.8	Red filter to view the fringes is required. Warm-up time is about 10 min.

used in these different spectral lamps. Even an ordinary fluorescent lamp with a plastic or glass green filter in front of the lamp works, but the fringe visibility is not high.

1.2.3. Materials for the Optical Flats

The optical flats are generally made of glass, fused silica, or more recently developed zero expansion materials such as CerVit and ULE glass. Small optical flats of less than 5 cm in diameter can be made of glass; they reach homogeneous temperature conditions reasonably quickly after some handling. It is preferable to make optical flats of larger sizes from fused silica or zero expansion materials. Table 1.3 gives relevant information regarding the materials commonly used for making optical flats.

When making a reference optical flat, it is necessary to consider carefully not only the material to be used but also the weight, size, testing methods, and many other important parameters (Primak 1984, 1989a, 1989b; Schulz and Schwider 1987).

1.2.4. Simple Procedure for Estimating Peak Error

Generally, optical surfaces are made to an accuracy ranging from a peak error of 2λ on the lower accuracy side to $\lambda/100$ on the higher side. It is possible by means of the

TABLE 1.3. Materials used for making optical flats and their properties.

Serial number	Material	Coefficient of linear expansion (per °C)	Remarks
1	BK7, BSC	$75\text{–}80 \times 10^{-7}$	These are borosilicate glasses that can be obtained with a high degree of homogeneity.
2	Pyrex	$25\text{–}30 \times 10^{-7}$	This is also a borosilicate glass but has higher silica content. Several manufacturers make similar type of glass under different brand names. This is a good material for making general quality optical flats and test plates.
3	Fused silica or quartz	6×10^{-7}	This is generally the best quartz material for making optical flats. Different grades of the material are available, based mainly on the degree of homogeneity.
4	CerVit, Zerodur	$0\text{–}1 \times 10^{-7}$	This material and similar ones made by different companies under different trade names have practically zero expansion at normal ambient temperatures.
5	ULE fused silica	$0\text{–}1 \times 10^{-7}$	This is a mixture of silica with about 7% titania.

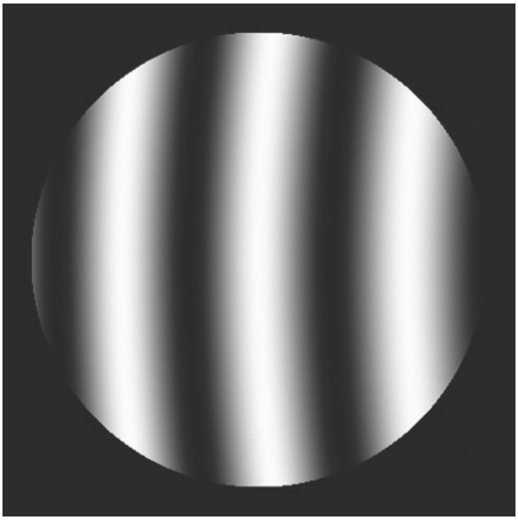

FIGURE 1.11. Newton fringes for an optical flat showing peak error of $\lambda/20$.

Newton interferometer to estimate peak errors up to about $\lambda/10$ by visual observation alone. Beyond that, it is advisable to obtain a photograph of the fringe system and to make measurements on this photograph. Figure 1.11 shows a typical interferogram as viewed in a Newton interferometer. Here, we have a peak error much less than $\lambda/4$. Consequently, the top plate is tilted slightly to obtain the almost straight fringes. The central diametral fringe is observed against a straight reference line such as the reference grid kept in the Newton interferometer in Figure 1.2. By means of this grid of straight lines, it is possible to estimate the deviation of the fringe from its straightness and also from the fringe spacing. The optical path difference is $2t$, so the separation between two consecutive fringes implies a change in the value of t equal to $\lambda/2$. Thus, if the maximum fringe deviation from the straightness of the fringes is d/k with d being the fringe separation, the peak error is given by

$$Peak\ error = \left(\frac{k}{d}\right)\left(\frac{\lambda}{2}\right) \tag{1.14}$$

In Figure 1.11 $k = 2.5$ mm and $d = 25$ mm; hence, we can say that the peak error is $\lambda/20$. Even in this case, it is desirable to know whether the surface is convex or concave, and for this purpose we can use the procedure described earlier. The only difference is that we have to imagine the center of the fringe system to be outside the aperture of the two flats in contact.

1.2.5. Measurement of Spherical Surfaces

Probably one of the most common applications of the Newton interferometer is the testing of the faces of small lenses while they are being polished. A small test plate

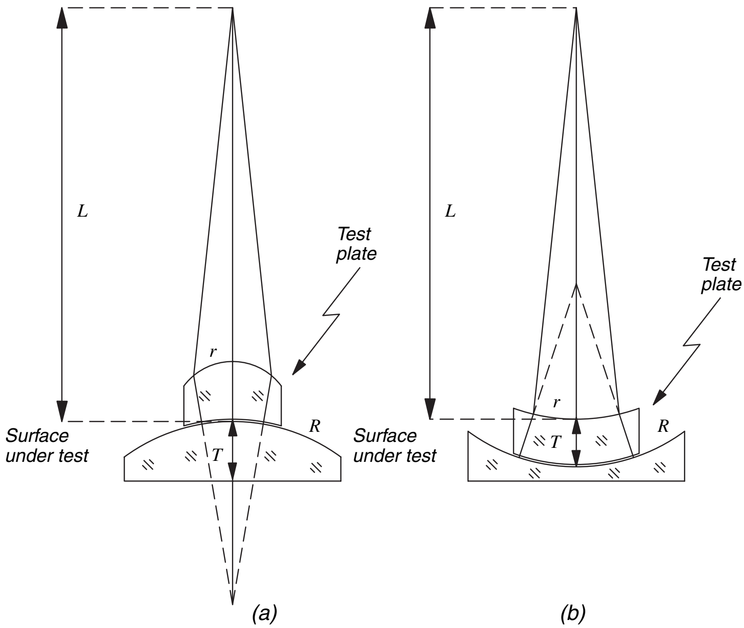

FIGURE 1.12. Test plates to test spherical surfaces with Newton fringes.

with the opposite radius of curvature is made according to the required accuracy and then placed over the surface under test. A test plate is useful not only to detect surface irregularities but also to check the deviation of the radius of curvature from the desired value (Karow 1979).

The observation should be made in such a way that the light is reflected almost perpendicular to the interferometer surfaces. Convex surfaces can be tested with the test plate shown in Figure 1.12(a), with a radius of curvature r in the upper surface given by

$$r = \frac{(N-1)(R+T)L}{NL+R+T}, \tag{1.15}$$

where N is the refractive index of the test plate glass. Concave surfaces can be tested as in Figure 1.12 (b). In this case, the radius of curvature r of the upper surface is

$$r = \frac{(N-1)(R-T)L}{NL-R+T} \tag{1.16}$$

It is important to remember that the fringes are localized very near to the interferometer surfaces, and therefore the eye should be focused at that plane.

The radius of curvature is checked by counting the number of circular fringes. The relation between the deviation in the radius of curvature and the number of rings can be derived with the help of Figure 1.13, where it can be shown that the distance

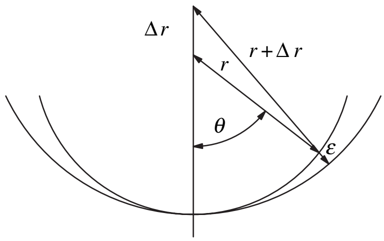

FIGURE 1.13. Geometry to find the separation between two spherical surfaces with different radii of curvature measured along the radius of one of them.

ε between the two surfaces, measured perpendicularly to one of the surfaces, is given by

$$\varepsilon = (r + \Delta r)\left\{1 - \left[1 - \frac{2(1 - \cos\theta)r\Delta r}{(r + \Delta r)^2}\right]^{1/2}\right\}. \tag{1.17}$$

If either Δr or the angle θ is small, this expression may be accurately represented by

$$\varepsilon = (1 - \cos\theta)\Delta r. \tag{1.18}$$

Since the number of fringes n is given by $n = 2\varepsilon/\lambda$, we can also write

$$\frac{n}{\Delta r} = \frac{2(1 - \cos\theta)}{\lambda} \tag{1.19}$$

If D is the diameter of the surface, the angle θ is defined as $\sin\theta = D/2r$. Therefore, a relation can be established between the increment per ring in the radius of curvature and the surface ratio r/D, as shown in Table 1.4.

1.2.6. Measurement of Aspheric Surfaces

Malacara and Cornejo (1970) used the method of Newton fringes to determine the aspheric profile of a surface that deviates markedly from a spherical surface. This method is useful if the aspheric deviates from the nearest spherical by a few wavelengths of light (say, 10–20λ). The method consists in using a spherical test plate in contact with the aspherical surface and finding the position of the fringes by means of a measuring microscope. From these position values, one can then obtain the actual air gap as a function of the distance, and a plot can be made and compared with the required aspheric plot. Figure 1.14 shows a typical schematic arrangement for this method.

It is important to consider that the surface under test probably does not have rotational symmetry. Therefore, the measurements must be made along several diameters in order to obtain the complete information about the whole surface.

TABLE 1.4. Radius of curvature increment per fringe for several values of the power ratio r/D of the spherical surface being tested with newton fringes.

r/D	$\Delta r/n$ (cm)
1.0	0.00020
2.0	0.00086
3.0	0.00195
4.0	0.00348
5.0	0.00545
6.0	0.00785
7.0	0.01069
8.0	0.01397
9.0	0.01768
10.0	0.02183
20.0	0.08736
30.0	0.19661
40.0	0.34970
50.0	0.54666
60.0	0.78712
70.0	1.07033
80.0	1.39665
90.0	1.77559
100.0	2.18144

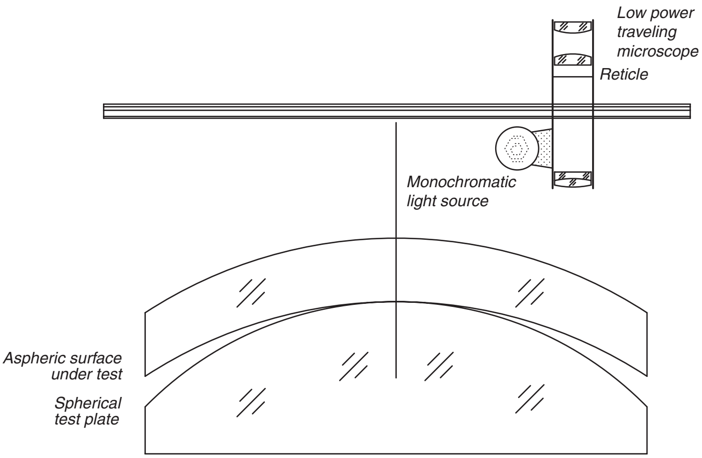

FIGURE 1.14. Schematic arrangement showing the method of measuring aspheric surfaces with a spherical test plate using Newton fringes.

Instead of directly measuring the fringe positions with a microscope, a photograph can be taken, and then the fringe positions can be measured with more conventional procedures.

If the reference surface is spherical and the surface under test is aspherical (hyperboloid or paraboloid), the ideal fringe patterns will be those of a Twyman–Green interferometer for spherical aberration as described in Chapter 2.

The reference surface may also be another aspherical surface that exactly matches the ideal configuration of the surface under test. This procedure is useful when a convex aspheric is to be made, since a concave aspheric can be made and tested more easily than a convex surface. The advantage of this method is that a null test is obtained. It has the disadvantage that the relative centering of the surfaces is very critical because both surfaces have well-defined axes, and these must coincide while testing. This problem is not serious, however, because the centering can be achieved with some experience and with some device that permits careful adjustment.

When mathematically interpreting the interferograms, it should be remembered that the OPD is measured perpendicularly to the surfaces, whereas the surface sagitta z is given along the optical axis. Therefore the OPD is given by $2(z_1 - z_2)\cos\theta$, where $\sin\theta = Sc$.

1.2.7. Measurement of Flatness of Opaque Surfaces

Sometimes we encounter plane surfaces generated on such metal substrates as steel, brass, and copper. An optical flat made of glass should be put on top of such objects for viewing Newton fringes. It is not always the case that the metal object is in the form of a parallel plate. The plane surface may be generated on an otherwise irregular component, and hence some means of holding the component while testing becomes necessary. This can be avoided if we can put the object on top of the optical flat and observe the fringes through the bottom side of the flat. This sort of arrangement is shown in Figure 1.15. Since most metal surfaces have reflectivities that are quite high compared to the value for a glass surface, the contrast of the fringes is not very good. To improve this situation, the optical flat is coated with a thin evaporated film of chromium or inconel having a reflectivity of about 30–40%. This brings about the formation of sharper, more visible fringes.

It is necessary to point out that if the object is very heavy, it will bend the optical flat and the measurement will not be accurate. Therefore, this kind of arrangement is suitable for testing only small, light opaque objects. In dealing with heavy objects, it is preferable to place the optical flat on top of the object.

1.3. FIZEAU INTERFEROMETER

In the Newton interferometer, the air gap between the surfaces is very small, and of the order of a few wavelengths of light. Sometimes it is convenient to obtain fringes similar to the ones obtained in the Newton interferometer, but with a much larger air gap. When the air gap is larger, the surfaces need not be cleaned as thoroughly as they

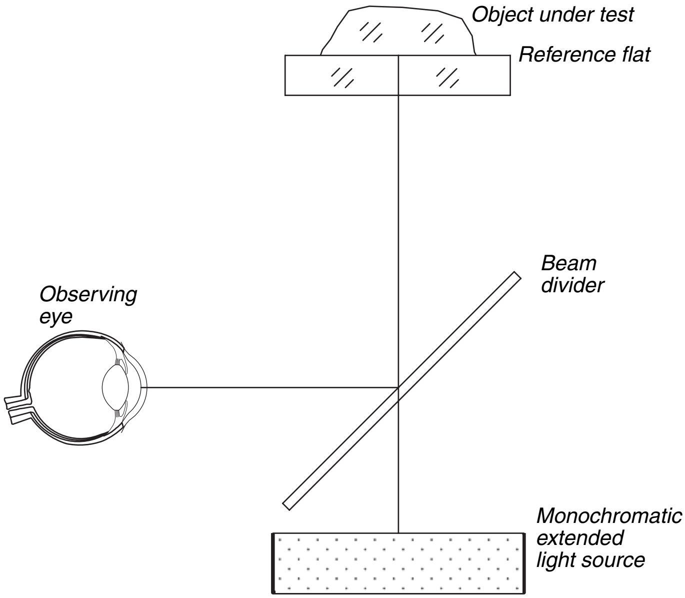

FIGURE 1.15. Schematic arrangement showing the method of testing opaque plane surfaces on irregular objects by placing them on top of the optical flat.

must be before being tested in the Newton interferometer. Also, due to the larger gap, the requirements for the collimation and size of the light source become stronger. This is called a Fizeau interferometer.

The Fizeau interferometer is one of the most popular instruments for testing optical elements. Some of its main applications will be described here, but the basic configurations used for most typical optical elements are identical to the ones used with the Twyman-Green interferometer to be described in Chapter 2. The reader is referred to that chapter for more details.

1.3.1. The Basic Fizeau Interferometer

From the foregoing considerations, it is seen that we should have a collimating system and a smaller light source in a Fizeau interferometer. Figure 1.16 shows the schematic arrangement of a Fizeau interferometer using a lens for collimation. The optical flat that serves as the reference is generally mounted along with the lens and is preadjusted so that the image of the pinhole reflected by the reference surface falls on the pinhole itself. Either the back side of the flat is antireflection coated or (more conveniently) the reference optical flat is made in the form of a wedge (about 10–20 min of arc) so that the reflection from the back surface can be isolated. To view the fringes, a beam divider is located close to the pinhole. The surface under test is kept below the reference flat, and the air gap is adjusted to the smallest value possible; then the air wedge is gradually reduced by manipulating the flat under test. When the air wedge is very large, two distinct images of the pinhole by the two surfaces can be

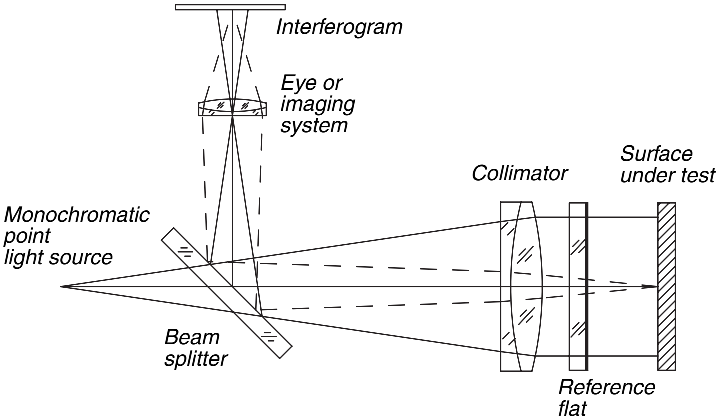

FIGURE 1.16. Schematic arrangement of a Fizeau interferometer using a lens for collimation of light.

seen in the plane P in Figure 1.16. By making use of screws provided to tilt the flat under test, one can observe the movement of the image of the pinhole and can stop when it coincides with that of the reference flat. Then the observer places his eye at the plane P and sees, localized at the air gap, the fringes due to variation in the air gap thickness. Further adjustment, while looking at the fringes, can be made to alter the number and direction of the fringes. The interpretation of these fringes is exactly the same as that for Newton and Twyman-Green fringes.

Figure 1.17 is a schematic of a Fizeau interferometer using a concave mirror as the collimating element. If a long focal length is chosen for the concave mirror, a spherical mirror can be used. For shorter focal lengths, an off-axis paraboloidal

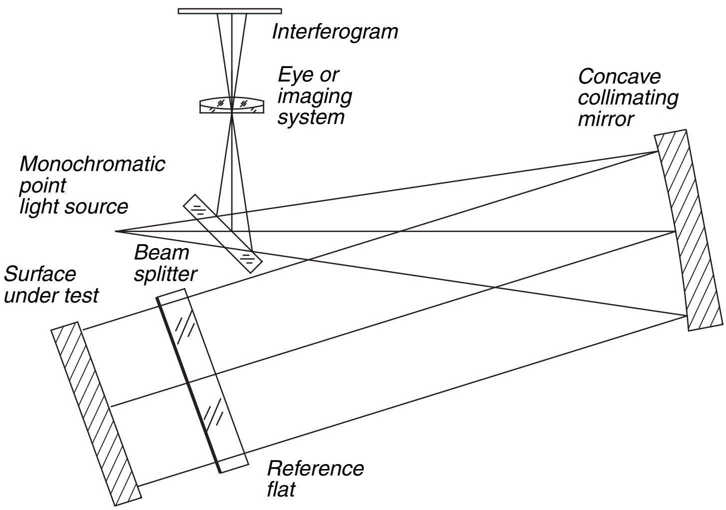

FIGURE 1.17. Schematic arrangement of a Fizeau interferometer using a concave mirror for collimation of the illuminating beam.

mirror may be required. Both the schemes of Figures 1.16 and 1.17 may be arranged in either a vertical (upright and inverted) or a horizontal layout. In the vertical situation the optical flats are horizontal, whereas in the horizontal layout the optical flats stand on their edges.

If the optical system or element under test has a high reflectivity and the reference flat is not coated, then the two interfering beams will have quite different intensities, and thus the fringes will have a poor contrast. On the contrary, if the reference flat is coated with a high reflectivity, but smaller than 100% to allow some light to be transmitted, a confusing system of fringes will appear because of multiple reflections. Commonly, to obtain two-beam interference fringes effectively, the reference surface must be uncoated. Then, to match the intensities, either the reflectivity of the optical element under test also has to be low or the amplitude of the beam under test has to be attenuated. The fact that the two surfaces reflecting the interfering beams have a low reflectivity makes it very important to take all necessary precautions to avoid spurious reflections at some other surfaces, mainly when a laser light source is used.

1.3.2. Coherence Requirements for the Light Source

As in the Newton interferometer, in the Fizeau interferometer the maximum allowed angular size of the light source to be used depends on the length of the air gap. For instance, if the air gap between the flats is 5 mm, and taking $\lambda = 5 \times 10^{-4}$ mm, the permissible value of 2θ given by Eq. (1.12) is 0.01 rad. Such a small angle can be obtained by using a collimator with the entrance pupil of the observer located at the focus, to observe the angle almost perpendicularly to the air gap for all points of the observed flats. Also, either the pupil of the observer or the light source has to be extremely small. Frequently the pupil of the eye has a diameter larger than required, so that it is simpler to have a light source with a pinhole. The larger the air gap is, the smaller the pinhole has to be.

When plane surfaces are tested in the Fizeau interferometer the air gap can be made quite small if desired. The total optical path difference involved does not exceed a few millimeters. Thus, a small low-pressure mercury vapor lamp can be used with a green filter as the source of light. When testing for the wedge of thick plates of glass, the OPD is larger due to the thickness. For gas or metal vapor lamp, this OPD is about the maximum we can use. For plates of greater thickness, the contrast of the interference fringes is greatly reduced because the lamp does not give a very sharp spectral line with a large temporal coherence. Similarly, the same situation of low contrast occurs when thick glass shells are tested or when spherical test plates are tested with one test plate.

This limitation can be eliminated, however, if we can use a source of very high monochromaticity. Fortunately, such a source, the laser, has recently become available. For our application, the low-power (2 mW) helium–neon gas laser operating in a single mode TEMoo and with a wavelength of emission at 632.8 nm is ideal. With this as the source of light, we can tolerate an OPD of at least 2 m and obtain Fizeau fringes of high contrast. Even larger OPDs are possible provided that a properly stabilized laser is chosen and vibration isolation is provided for the instrument.

Most of the coherence requirements for Fizeau interferometers are similar to the requirements for Twyman–Green interferometers as described in section 2.3. There, it is pointed out that a gas laser has perfect spatial coherence, and can have almost perfect temporal coherence and thus we might think that this is the ideal light source for interferometry, but this is not always the case. The reason is that many unwanted reflections from other surfaces in the optical system may produce a lot of spurious fringes that can appear. Also, the laser light produces scattering waves from many small pieces of dust or scratches in the optical elements. To solve this problem, the light source can be extended even when using a laser by introducing a thin rotatory half ground glass close to the point light source. Deck et al. (2000) have proposed an annular shape for the light source by using a diffracting element to produce a small cone of light illuminating the rotating ground glass. The effect of the spurious reflections has been studied by several researchers, for example by Ai and Wyant (1988 and 1993) and by Novak and Wyant (1997).

Another possible effect to be taken into account is that some optical elements or systems to be tested may be retroreflectors, either in one dimension like a porro prism, or in two dimensions like a cube corner prism. The retroreflection has associated an inversal, reversal, or both (which is equivalent to a 180° rotation) of the wavefront. A point of view is that then the interference takes place between two different points on the wavefront, symmetrically placed with respect to the optical axis if the wavefront was rotated, or symmetrically placed with respect to the inversion or reversion axis. The fringes will have a good contrast only if the spatial coherence of the wavefront is high enough. This condition imposes a stronger requirement on the small size of the point light source.

Another equivalent explanation for this retroreflection effect is illustrated in Figure 1.18. Let us consider the pinhole on the light source to have a small finite

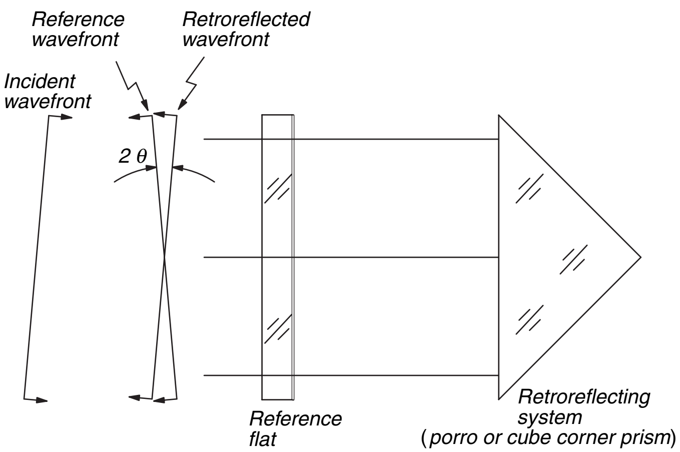

FIGURE 1.18. Interference between the reference wavefront and the wavefront retroreflected by a porro prism under test. Both wavefronts originate at one point on the edge of the small light source. The angle between these two wavefronts reduces the contrast of the fringes.

size and a flat collimated incidence wavefront coming from the edge of that pinhole at a small angle θ. It is easy to see that the two interfering wavefronts will not be parallel to each other, but will make an angle 2θ between them. Of course, there are infinite number of wavefronts coming from different points at the pinhole of the light source, all with different orientations and angles, smaller than θ. This multiplicity of wavefronts with different angles will reduce the contrast of the fringes from a maximum at the center where all the wavefronts intersect, decreasing towards the edge of the pupil. This effect is also present for the same reason in the Twyman–Green interferometer as described in Chapter 2 in more detail.

The strong spatial coherence requirements when a retroreflecting system is tested is difficult to satisfy with gas or metal vapor lamps, but with gas lasers it is always fulfilled.

1.3.3. Quality of Collimation Lens Required

We shall briefly examine the quality of collimating lens required for the Fizeau interferometer. Basically, we are interested in determining the variation in air gap thickness. However, the OPD is a function of not only the air gap thickness but also the angle of illumination, and at a particular point this is $2t\cos\theta$. The air gap t varies because of the surface defects of the flats under test, while the variation of θ is due to the finite size of the source and the aberration of the collimating lens.

For Fizeau interferometers using conventional sources of light, the maximum air gap that is useful is 50 mm. Also, in this case we have to consider the size of the source and the aberration of the lens separately. The effect of the size of the source is mainly on the visibility of the Fizeau fringes. The excess optical path difference $t\theta^2$ should be less than $\lambda/4$ for good contrast of the Fizeau fringes and the pinhole is chosen to satisfy this condition. The effect of the pinhole is uniform over the entire area of the Fizeau fringes. On the contrary, the effect of aberration in the collimating lens is not uniform. Thus, we have to consider the angular aberration of the lens and its effect. If ϕ is the maximum angular aberration of the lens, then $t\phi^2$ should be less than $k\lambda$, where k is a small fraction that depends on the accuracy required in the instrument. Thus, let us set $k = 0.001$, so that the contribution of $t\phi^2$ is 0.001λ. Taking a maximum value of $t = 50$ mm for the ordinary source situation, we have

$$\phi^2 \leq \frac{0.001\lambda}{t} \approx 10^{-8},$$

or

$$\phi = 10^{-4} \text{ rad.} \tag{1.20}$$

This angular aberration is quite large, being of the order of 20 s of arc. Hence, suitable lenses or mirror systems can be designed for the purpose (Taylor, 1957; Yoder, 1957; Murty and Shukla, 1970).

1.3.4. Liquid Reference Flats

It is well known that a liquid surface can be used as a reference flat. Basically the liquid surface has a radius of curvature equal to that of the earth. If the radius of the earth is taken as 6400 km, the sag of the surface is (Grigor'ev et al., 1986; Ketelsen and Anderson 1988)

$$\frac{y^2}{2R} = \frac{y^2}{2 \times 6.4 \times 10^{-9}} \text{ mm} \tag{1.21}$$

where $2y$ is the diameter of the liquid surface considered. If we stipulate that this should not exceed $\lambda/100$ ($\lambda = 5 \times 10^{-4}$), then

$$y^2 \leq 6.4 \times 10^4$$

or

$$2y \leq 512 \text{ mm} \tag{1.22}$$

Thus, a liquid surface of about 0.5 m diameter has a peak error of only $\lambda/100$ as compared to an ideal flat. Therefore, it has been a very attractive proposition to build liquid flats as standard references. In practice, however, there are many problems, mainly in isolating the disturbing influence of vibrations. It is also necessary to exclude the region near the wall of the vessel that holds the liquid and to make sure that no dust particles are settling down on the surface. Possible liquids that can be useful for the purpose are clear and viscous, such as glycerin, certain mineral oils, and bleached castor oil. Water is probably not suitable because of its low viscosity. Mercury may not be suitable because of its high reflectivity; the two interfering beams will have very unequal intensities, resulting in poor contrast of the fringes unless the surface under test is also suitably coated. However, mercury has been used as a true horizontal reference plane reflecting surface in certain surveying and astronomical instruments.

1.3.5. Fizeau Interferometer with Laser Source

We shall now describe a Fizeau interferometer using a source such as the helium–neon gas laser of about 2 mW power lasing at 632.8 nm in the single mode. A schematic diagram is shown in Figure 1.19. A very well corrected objective serves to collimate the light from the pinhole, illuminated by a combination of the laser and a microscope objective. Between the collimating objective and the pinhole (spatial filter), a beam divider is placed so that the fringes can be observed from the side. It is also desirable to provide a screen, upon which the Fizeau fringes are projected, to avoid looking into the instrument as is normally done when conventional light sources are used. The laser has a high radiance compared to other sources, and a direct view may be dangerous to the eye under some circumstances. The reference

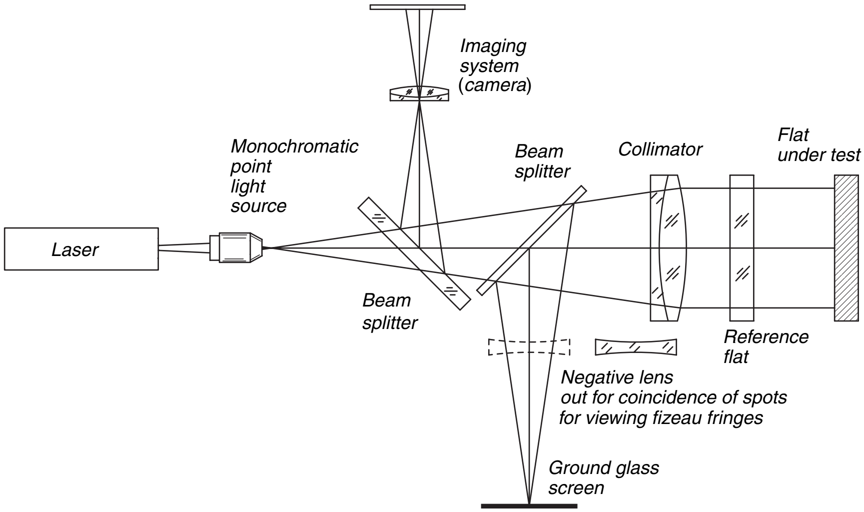

FIGURE 1.19. Schematic arrangement of a Fizeau interferometer using a laser source. The scheme shown here is for plane surfaces. The system is easily aligned with the help of a sliding negative lens.

plane surface is permanently adjusted so that the reflected image of the pinhole is autocollimated. The surface under test is adjusted until the image reflected from it also comes into coincidence with the pinhole. To facilitate preliminary adjustment, the screen is used to project the two pinhole images from the two reflecting plane surfaces. This is accomplished by removing the negative lens between the beam divider and the ground glass screen. The pinhole image from the reference surface is at the center of the screen, whereas the one from the surface under test is somewhere on the screen; by manipulation of this surface, the two spots of light on the screen can be brought into coincidence. Then the negative lens is inserted in the path, and the Fizeau fringes are projected on the screen. These fringes can be further adjusted in direction and number as required. By the use of another beam divider, it is possible to divert part of the beam to a camera for taking a photograph of the fringe pattern. The whole instrument must be mounted on a suitable vibration-isolated platform.

This instrument can be used for various other applications that are normally not possible with conventional sources of light. We describe some such applications in the sections that follow. In addition, many possibilities exist for other applications depending on the particular situations involved.

Several commercial Fizeau interferometers have been available for several years, but probably the two most widely known are the Zygo interferometer (Forman, 1979), shown in Figure 1.20, and the Wyko interferometer, shown in Figure 1.21.

1.3.6. Multiple-Beam Fizeau Setup

If, instead of two-beam fringes, multiple-beam fringes of very good sharpness are required, the reference optical flat and the optical flat under test are coated with a

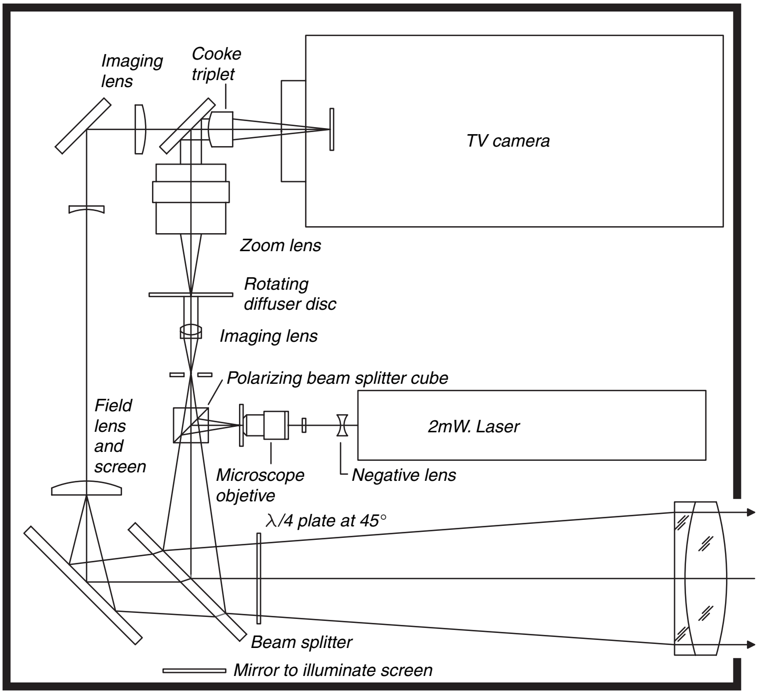

FIGURE 1.20. Fizeau interferometer manufactured by Zygo Corp. (Courtesy of Zigo Corp.).

reflecting material of about 80–90% reflectivity (see Chapter 6) such as aluminum or silver. If higher reflectivities are required, multilayer dielectric coatings can be applied. In fact, the instrument may be provided with several reference flats having coatings of different reflectivities.

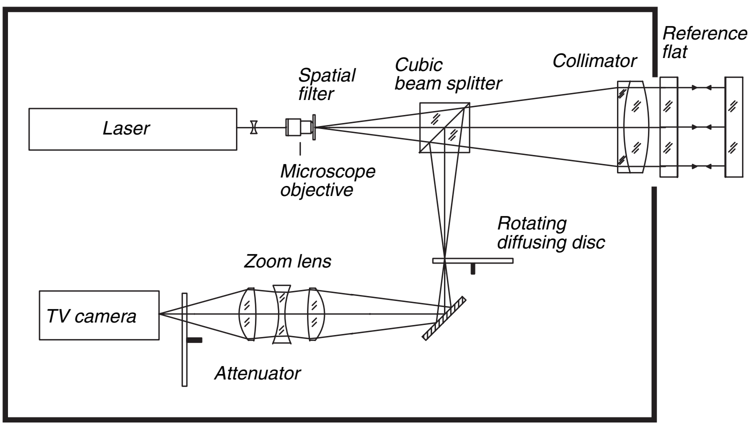

FIGURE 1.21. Fizeau interferometer manufactured by Wyko Corp. (Courtesy of Wyko Corp.).

1.3.7. Testing Nearly Parallel Plates

In many applications, glass plates having surfaces that are both plane and parallel are required. In such cases, the small wedge angle of the plate can be determined by the Fizeau interferometer, and the reference flat of the interferometer need not be used since the fringes are formed between the surfaces of the plate being tested. If α is the angle of the wedge and N is the refractive index of the glass, the angle between the front- and back-reflected wavefronts is given by $2n\alpha$, and hence the fringes can be expressed as

$$2N\alpha = \frac{\lambda}{d}, \tag{1.23}$$

where d is the distance between two consecutive bright or dark fringes. Hence the angle α is given by

$$\alpha = \frac{\lambda}{2nd}. \tag{1.24}$$

To determine the thinner side of the wedge, a simple method is to touch the plate with a hot rod or even with a finger. Because of the slight local expansion, the thickness of the plate increases slightly. Hence a straight fringe passing through the region will form a kink pointing toward the thin side, as shown in Figure 1.22. For instance, if we take $N = 1.5$, $\lambda = 5 \times 10^{-4}$ mm, and $\alpha = 5 \times 10^{-6}$ (1 s of arc), we get for d a value of about 33 mm. Hence a plate of 33 mm diameter, showing one fringe, has a wedge angle of 1 s of arc. If the plate also has some surface errors, we

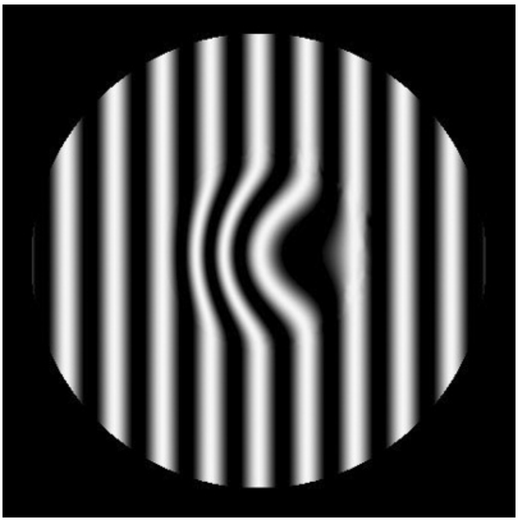

FIGURE 1.22. Kink formation in the straight Fizeau fringes of a slightly wedged plate, obtained by locally heating the plate. The kink is pointing toward the thin side of the wedge.

get curved fringes, indicating both surface and wedge errors. If the surfaces are independently tested and found to be flat, and even in this situation one is getting curved fringes, these should be attributed to variation of the refractive index inside the plate in an irregular manner. In fact, by combining the tests on the Newton interferometer and the Fizeau interferometer for a parallel plate, it is possible to evaluate the refractive index variation (inhomogeneity) (Murty, 1963; Murty, 1964a; Forman, 1964).

1.3.8. Testing the Inhomogeneity of Large Glass or Fused Quartz Samples

The sample is made in the form of a parallel plate. The surfaces should be made as flat as possible with a peak error of not more than λ. Then the plate is sandwiched between two well-made parallel plates of glass with a suitable oil matching the refractive index of the sample. This will make the small surface errors of the sample negligible, and only straight fringe deformation due to the inhomogeneity of the sample will be seen. If the sandwich is kept in the cavity formed by the two coated mirrors, very sharp dark fringes on a bright background are obtained. If, for instance, the maximum fringe deviation from straightness is k and the distance between two fringes is d, the optical path difference is $(k/d)\lambda$. Now the OPD due to the inhomogeneity ΔN and thickness t of the sample is given by $2\Delta N \cdot t$, and hence

$$\Delta N = \left(\frac{k}{d}\right)\left(\frac{\lambda}{2t}\right) \tag{1.25}$$

As an example, if $k/d = 0.25$, $\lambda = 632.8\,\text{nm}$, and $t = 50\,\text{mm}$, we have $\Delta N = 1.6 \times 10^{-6}$. Thus a maximum variation of 1.6×10^{-6} may be expected in the sample for the direction in which it has been tested. Figure 1.23 shows the schematic arrangement of the Fizeau interferometer for the method just described.

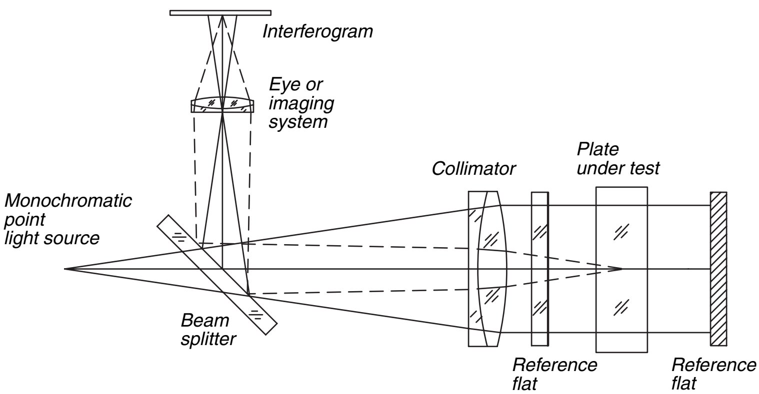

FIGURE 1.23. Schematic arrangement of a Fizeau interferometer for testing the homogeneity of solid samples of glass, fused quartz, and so on.

1.3.9. Testing the Parallelism and Flatness of the Faces of Rods, Bars, and Plates

Frequently, the need for testing the parallelism and the flatness of two opposite faces in a rod, plate, or bar arises. If the plate to be tested is transparent and has a highly homogeneous refractive index, the problem is not so complicated. If the refractive index of the material is inhomogeneous or if it is not transparent, special techniques have to be developed.

Vannoni and Molezini (2004) described a configuration for this purpose, as illustrated in Figure 1.24. The first step is to adjust the interferometer to produce the minimum number of fringes without the plate or rod to be tested. The field of view will show the fringes due to any possible defect in the right angle prism. Then the plate is inserted as shown in the figure.

1.3.10. Testing Cube Corner and Right-Angle Prisms

In their retro-reflective configuration, if the right angles of cube comer and right-angle prisms are exact without any error, they reflect an incident plane wavefront as a single emerging plane wavefront. Otherwise the reflected wavefront consists of several plane wavefronts with different tilts, making possible the measurement of the prism errors. Because of the total internal reflection, the intensity of reflected light from these prisms is very high, nearly 100%. Since the reference flat is not coated, the fringes will have a poor contrast. To optimize the fringe contrast, either the reflectivity of the optical element under test also has to be low or the amplitude of the beam under test has to be attenuated.

To reduce the effective reflectivity of the right angle or cube prism, we can introduce a parallel plate of glass coated with a metallic film having a transmission between 20% and 30%. In this case the intensities of the two beams matched reasonably well, and we get a good contrast of two-beam fringes. The coated plate between the prism and the uncoated reference flat should be tilted

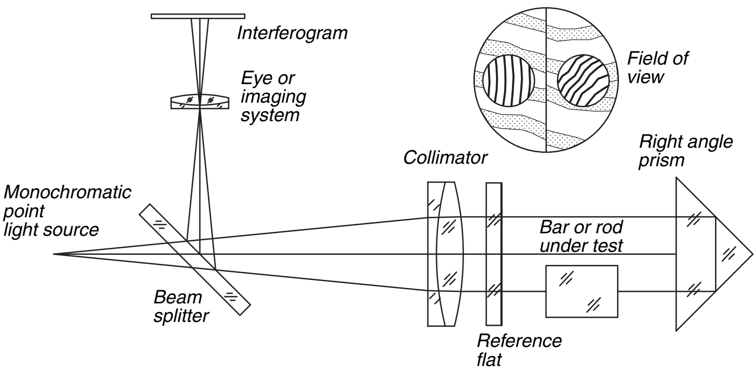

FIGURE 1.24. Schematic arrangement to test an opaque bar or rod for flatness and parallelism of the two opposite faces.

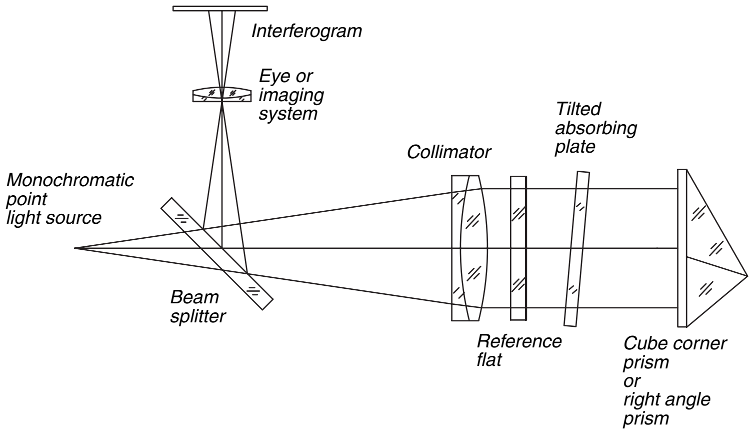

FIGURE 1.25. Schematic arrangement of a Fizeau interferometer for testing cube corner prisms and right-angle prisms. Here an absorbing plate is inserted between the prisms and the reference flat surface to equalize the intensities of the two interfering beams.

sufficiently to avoid the directly reflected beam. This method is shown schematically in Figure 1.25.

Another possible method is to reduce the reflectivity of one of the total reflecting surfaces. This can be done by constructing a special cell in which the prism is mounted, and behind one reflecting surface, a thin layer of water or some other suitable liquid is in contact with the surface. Thus, in effect, the refractive index difference is reduced at one total internal reflecting surface, and hence, the intensity of the wavefront reflected from the prism matches that of an uncoated flat. This method is shown schematically in Figure 1.26.

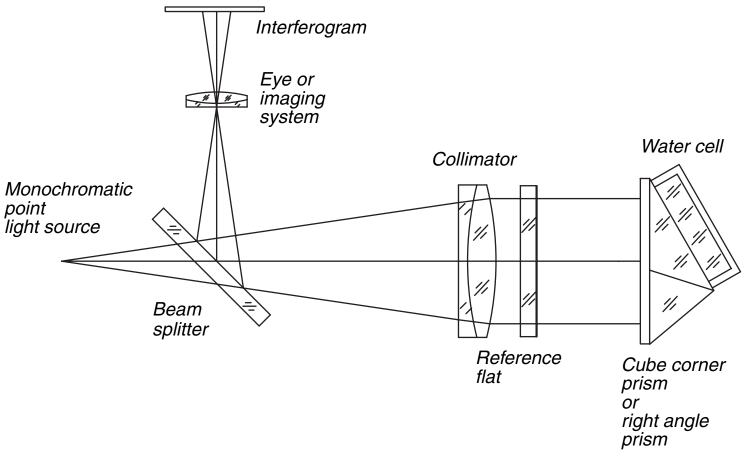

FIGURE 1.26. A scheme for reducing the intensity of reflected light from the corner cube prism and the right-angle prism. One of the total internally reflecting faces is brought into contact with water or some other liquid by the use of a cell behind it.

The interferograms obtained when testing of these prisms are identical to those in the Twyman–Green interferogram. For more details please see Chapter 2.

1.3.11. Fizeau Interferometer for Curved Surfaces

Just as collimated light is employed for testing optical flats on the Fizeau interferometer, it is possible to use either divergent or convergent light for testing curved surfaces. Figure 1.27 shows an arrangement for testing a concave surface against a reference convex surface. The point source of light is located at the center of the curvature of the convex reference surface. The concave surface under test is adjusted until its center of curvature, too, almost coincides with the point source of light. The procedure is exactly the same as before except that to achieve the uniform air gap, we have to provide some translational motion also (Moore and Slaymaker, 1980).

The same setup can be used very easily for checking the uniformity of the thickness (concentricity) of spherical shells. In this case the interfering beams are obtained from the front and back of the two spherical concentric surfaces. Figure 1.28 shows this setup for testing the concentricity of a spherical shell. If the radii of curvature are correct but the shell has a wedge (the centers of curvature are laterally displaced), we get straight fringes characteristic of the wedge. The hot rod or finger touch procedure described in Section 1.2.3 can be adopted to determine which side is thinner. If the two radii are not of proper value ($\sqrt{r_1 - r_2} \neq t$, where r_1 and r_2 are the two radii and t is the center thickness), the value of t is not constant over the entire shell. Hence, we get circular fringes like Newton fringes. If in addition a wedge is present, the center of these circular fringes will be decentered with respect to the center of the shell. In this situation also, we can adopt the hot rod or finger touch procedure to decide whether the shell is thin at the edge or at the center.

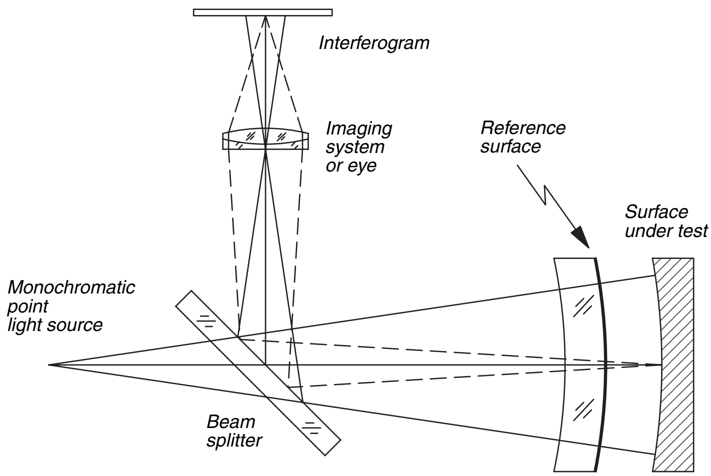

FIGURE 1.27. Fizeau interferometer set up for curved surfaces. Here the convex surface is the reference surface and the concave surface is under test.

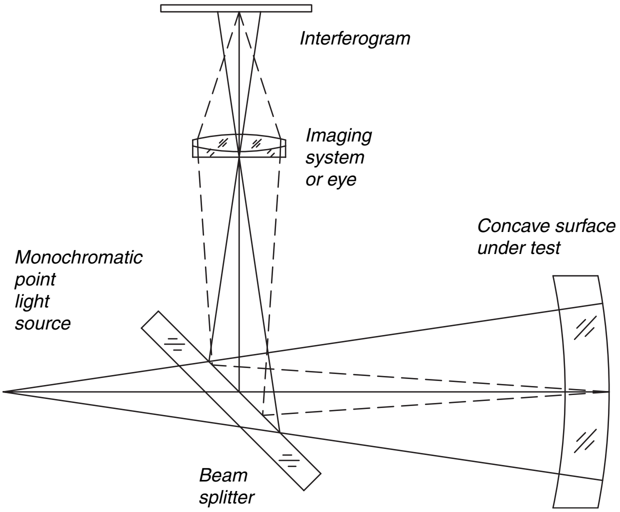

FIGURE 1.28. Fizeau interferometer setup for testing the concentricity of the spherical shell.

We can also have an arrangement for testing convex surfaces against a concave reference surface, as shown schematically in Figure 1.29. Here we use a lens or a group of lenses at finite conjugate distances such that the point source of light is at one conjugate, whereas the common center of curvature of the test surface and the reference surface is at the other conjugate. The concave reference surface is fixed to the instrument, while the convex surface under test is manipulated in the usual manner to obtain a uniform air gap.

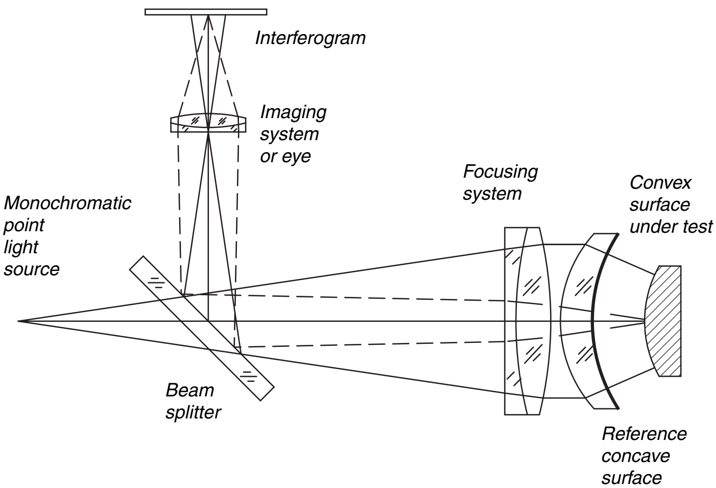

FIGURE 1.29. Fizeau interferometer setup for testing a convex surface against a concave reference surface.

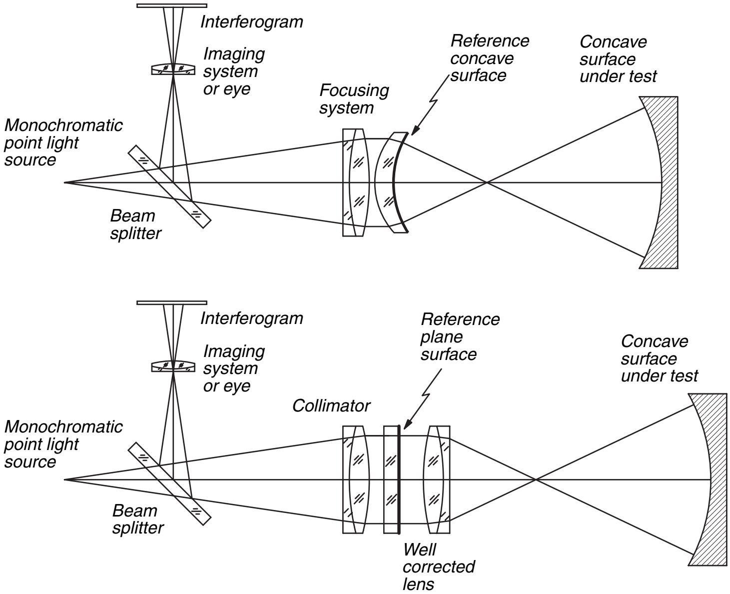

FIGURE 1.30. Schematic diagram of a Fizeau interferometer for testing a concave surface using a concave reference surface or a flat reference surface.

1.3.12. Testing Concave and Convex Surfaces

The reference surface is again the uncoated flat surface that is part of the Fizeau interferometer. The collimated light from the instrument, after passing through the optical flat, is again focused by the use of another highly corrected lens. If the surface is concave, it is set up as shown in Figure 1.30; if convex, as shown in Figure 1.31. When the surface is spherical and the center of curvature coincides with the focus of the lens, a plane wavefront is reflected back. Hence, we should obtain straight fringes due to the interference of the two beams. If the optical reference flat and the spherical surfaces are coated with high reflecting material, we can get very sharp, multiple-beam Fizeau fringes. If the surfaces are not spherical but are aspheric, appropriate null lenses must be used in the interferometer. This setup can also be used to measure the radius of curvature if a length-measuring arrangement is provided.

The testing of convex surfaces with the Fizeau interferometer presents many interesting problems, mainly if the surface is large and/or aspheric, which have been analyzed by several authors, for example by Burge (1995).

Another interferometer, which may be considered as a Fizeau interferometer, was devised by Shack (Shack and Hopkins, 1979; Smith, 1979). The difference is that this scheme uses a He–Ne laser source to give very large coherence length. Hence, the separation between the convex reference surface and the concave surface under test can be very large (typically several meters). Also, the convex reference surface

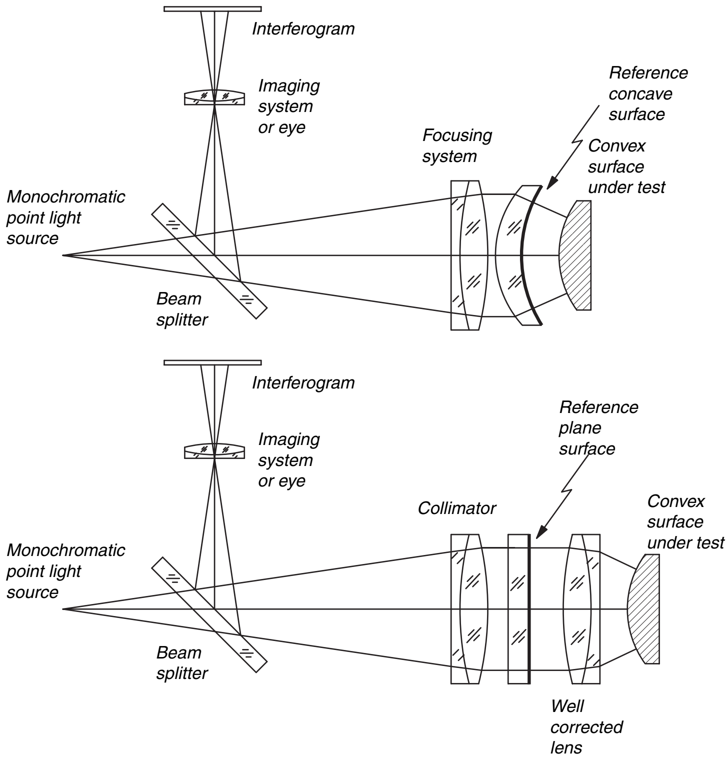

FIGURE 1.31. Schematic diagram of a Fizeau interferometer for testing a convex surface using a flat concave reference surface or a flat reference surface.

becomes a part of the instrument and can be of very short radius of curvature. The scheme, in fact, incorporates the device in the form of a beam-divider cube with one of the faces made into a convex spherical surface. The Shack interferometer is shown schematically in Figure 1.32. It is possible to test a large aspherical surface with this interferometer if a suitable null corrector is inserted between the interferometer and the surface under test.

1.4. HALDINGER INTERFEROMETER

With the Newton and Fizeau interferometers, we are basically interested in finding the variation in the air gap thickness. In these cases, the fringes are referred to as fringes of equal thickness. If, however, the thickness of the air gap is uniform and it is illuminated by a source of large angular size, we get what are called fringes of equal inclination. These fringes are formed at infinity, and a suitable lens can be used to focus them on its focal plane. If the parallel gap is that of air, we have the simple relation $2t \cos\theta = n\lambda$, as given in Eq. (1.9), from which we can easily see that, for a

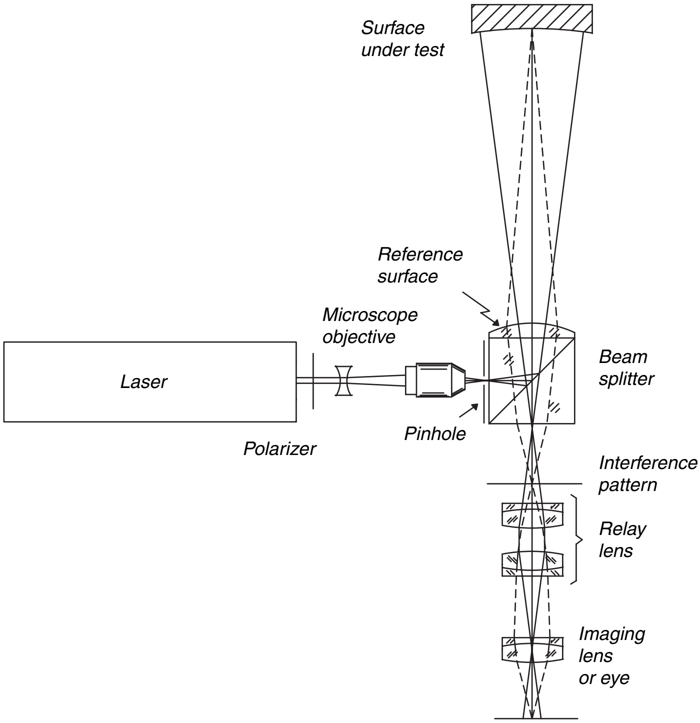

FIGURE 1.32. Schematics of a Shack–Fizeau interferometer.

constant value of t, we obtain fringes of equal inclination that are circles and are formed at infinity.

If the air gap is replaced by a solid plate such as a very good parallel plate of glass, Eq. (1.9) is modified slightly to include the effect of the refractive index N of the plate and becomes

$$2Nt\cos\theta' = n\lambda \tag{1.26}$$

where θ' is the angle of refraction inside the glass plate. For small values of θ', we may approximate this expression as

$$2Nt = \left(\frac{t}{N}\right)\theta^2 = n\lambda \tag{1.27}$$

To see Haidinger fringes with simple equipment, the following method, illustrated in Figure 1.33 may be adopted. A parallel plate of glass is kept on a black paper and is illuminated by the diffuse light reflected from a white card at 45°. At the center of the white card is a small hole through which we look at the plate. With relaxed accommodation our eyes are essentially focused at infinity, i, and we see a system

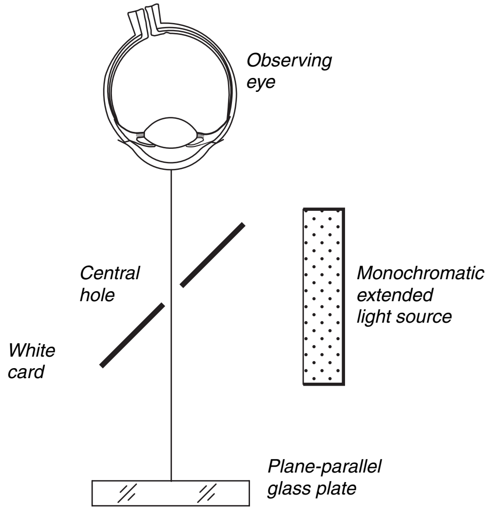

FIGURE 1.33. A simple arrangement to see Haidinger fringes for a nearly parallel glass plate.

of concentric circular fringes. For the light source we can use a sodium or even a fluorescent lamp.

In the situation where the laser is the source of light, there is a much higher limit for the value of t. Even though several meters can be used for t, we shall set $t = 1000\,\text{mm}$. In this case, using $\lambda = 632.8\,\text{nm}$, we get for ϕ an upper limit of 5 s of arc. Hence it is not difficult to design a collimating system to satisfy this condition.

Another aspect that is important, especially with large values of t, is the lateral shear one can get in the instrument. To avoid this, the autocollimated pinhole images must coincide with the pinhole itself. Similarly, if the collimating lens is not properly collimated, either a convergent or a divergent beam will emerge. The collimation may be accurately performed by using any of the various devices available, such as the plane parallel plate shearing interferometer (Murty, 1964b).

A somewhat better method is to use a lens for focusing the system of Haidinger fringes on its focal plane. This requires a setup almost identical to that for the Fizeau interferometer. The only difference is that, instead of a pinhole, a wider aperture is used to have a large angular size for the source. The Haidinger fringes are then formed in the focal plane of the lens.

1.4.1. Applications of Haidinger Fringes

The Haidinger fringes may be used as a complementary test to that provided by the Fizeau interferometer. If we are testing a nearly parallel plate, we can find its wedge angle either by the Fizeau or by the Haidinger method. In the Haidinger method we look for the stability of the concentric fringes as we move our line of sight across the plate with a small aperture. If t is slowly varying, the center of the circular fringe system also appears to change. If t is decreasing, we are moving toward the thinner side of the wedge, and in this case the circular Haidinger fringes appear to expand from the center. On the contrary, the fringes appear to converge to the center if we are moving toward the thick side of the wedge. If we note how many times the center of the fringe system has gone through bright and dark cycles, we can also estimate the wedge angle in the same manner as for the Fizeau situation.

1.4.2. Use of Laser Source for Haidinger Interferometer

A helium–neon laser source of low power is very useful for this interferometer, as it is for the Fizeau instrument. It enables the fringes to be projected on a screen. In this case, the laser can be made to give effectively a point source of light, and consequently, the Haidinger fringes can be considered as the interference from two point sources that are coherent to each other. Hence it is possible to obtain the circular fringes even at a finite distance from the two coherent point sources, and no lens is needed to form the fringes in its focal plane. Figure 1.34 shows the two point images of a point source reflected from a glass plate having a wedge. For the purpose of analysis, it is sufficient for us to consider two point sources of light that are coherent to each other. Then, if we place a screen sufficiently far away and perpendicular to the line joining the two sources, we get a system of concentric circular fringes similar to Newton's rings and the center of the fringes is collinear with the two point sources. Also, for a glass plate of refractive index N, the distance between the virtual point sources is $2t/N$, where t is the thickness of the plate. Now, if the glass plate has a small wedge, the two virtual sources will also have a slight lateral displacement with respect to each other; this is given by $2N\alpha r$, where α is the wedge angle and r is the distance of the point source from the wedged plate. These various parameters are illustrated in Figure 1.34.

To apply this theory in practice, several methods are available. One method, proposed by Wasilik et al. (1971), is illustrated in Figure 1.35. The laser beam is allowed to pass through a small hole in a white cardboard and is then incident on

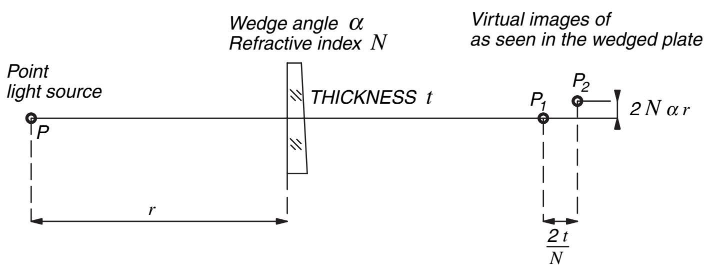

FIGURE 1.34. Various parameters related to the formation of two virtual coherent sources from a single point source by a wedged plate.

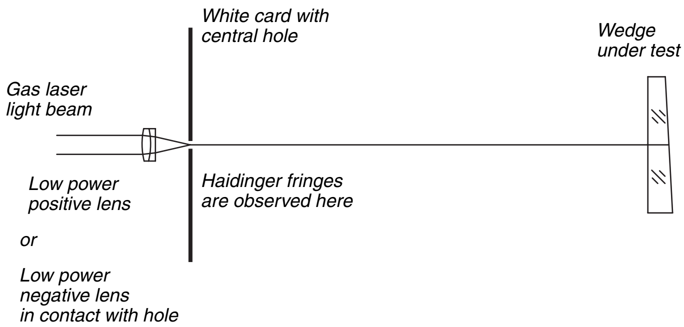

FIGURE 1.35. A schematic arrangement for observing the Haidinger fringes and measuring the displacement of the center. Here a laser beam is passed through a cardboard, and the Haidinger fringes are observed around the hole on the cardboard.

the glass plate under test. To provide some divergence for the laser beam, a negative or positive lens of about 50–100 mm focal length is introduced centrally behind the cardboard. The lens can be fixed in such a manner that it does not deviate the beam but only expands it slightly. This cardboard may be made specially, along with the lens, to fit on the laser. Several concentric circles with known spacing may be drawn on the cardboard for measuring purposes. The plate under test is kept on a platform that can be tilted. The plate is adjusted until the spot of laser light reflected from it goes back through the hole in the cardboard. In this situation concentric circular Haidinger fringes will be seen on the cardboard surrounding the hole. If the plate is free from the wedge, the center of the Haidinger fringe system coincides with the center of the hole. If the plate has a wedge, the center of the Haidinger fringe system is displaced with respect to the center of the hole. An approximate formula relating this displacement to the wedge angle of the wedged glass plate is as follows:

$$d = \frac{2N^2 r^2 \alpha}{t} \tag{1.28}$$

where $d =$ displacement of the Haidinger fringe system,
$\alpha =$ wedge angle of the plate,
$t =$ thickness of the glass plate,
$N =$ refractive index of the glass plate,
$r =$ distance of the point source from the glass plate.

For example, if $\alpha = 1\,\text{s}$ of arc $(5 \times 10^{-6}\,\text{rad})$, $N = 1.5$, $r = 1000\,\text{mm}$, and $t = 10\,\text{mm}$, we have $d = 2.25\,\text{mm}$, which can be easily detected. Hence this method is quite sensitive and useful.

Another method is illustrated in Figure 1.36. Here the laser beam passes through the wedged-glass plate and falls on a specially prepared ground-glass plate in the center of which a small concave or convex reflector of about

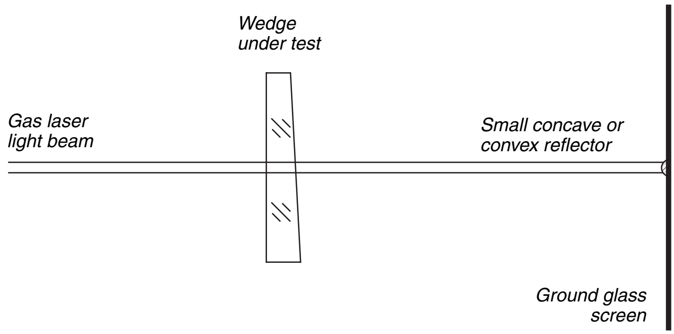

FIGURE 1.36. A schematic arrangement for observing the Haidinger fringes and measuring the displacement of the center. Here the laser beam is directed back into the wedged glass plate by a small concave or convex mirror on the ground glass. The Haidinger fringes are formed on the ground glass.

50–100 mm radius of curvature is cemented. The size of the reflector should be slightly greater than the spot size of the laser. Thus, the laser beam is reflected back onto the glass plate. The wedged plate is adjusted until the reflected spot from it coincides with the small reflecting mirror on the ground glass. Now, Haidinger fringes can be seen on the ground glass, and the center of the fringe system is displaced with respect to the mirror on the ground glass. The same formula, Eq. (1.28), is also valid for this case.

A third method utilizes a beam divider, as shown in Figure 1.37. The laser beam passes through the beam divider, which after reflection from the wedged plate is again reflected at the beam divider and finally falls on a ground-glass screen. The plate under test is adjusted until the laser spot reflected from it goes back on itself. After the position of the spot on the ground glass has been noted, a negative or positive lens is introduced into the laser beam close to the laser side. This widens the beam sufficiently so that circular Haidinger fringes can be seen on

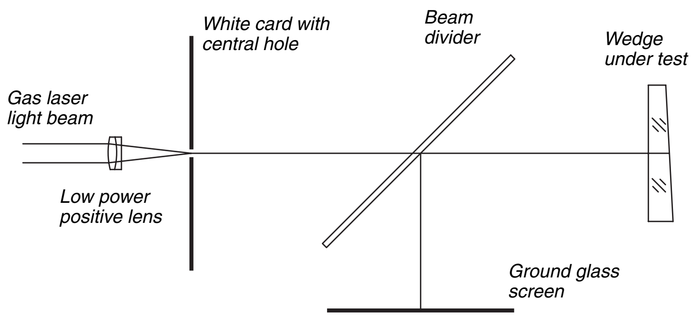

FIGURE 1.37. A schematic arrangement for observing the Haidinger fringes and measuring the displacement of the center. Here the fringes are observed on the ground glass and by means of a beam divider, the central obscuration is avoided.

the ground-glass screen. The displacement of the center of the Haidinger fringe system is measured, and the same formula, Eq. (1.28), can be used for calculating the wedge angle α.

1.4.3. Other Applications of Haidinger Fringes

We have discussed earlier the application of Haidinger fringes for the determination of the very small wedge angle of a nearly parallel plate of glass. There are many types of prisms that can be reduced to equivalent parallel plates and hence can be tested for deviation from their nominal angles. A typical example is a right-angle prism with nominal angles of 90°, 45°, and 45°. In such a prism, it is usually required that the 90° angle be very close to its nominal value and that the two 45° angles be equal to each other. In addition, all the faces of the prism should be perpendicular to a base plane. If not, we say that the prism has pyramidal error that is objectionable in many applications. Figure 1.38 shows how the right-angle prism can be treated as an equivalent parallel plate with a very small wedge angle. If the beam is incident first on the face AC, the beam returning after reflection from the face BC is nearly parallel to the one reflected from the face AC, and hence Haidinger fringes are seen as a result of the interference between these two beams. This arrangement checks the equality of the angles A and B. If there were no pyramidal error and the two angles are equal, the center of the Haidinger fringes will be exactly at the center of the beam spot. If the angles are equal but there is a pyramidal error, the center of the Haidinger fringes will be displaced vertically. If both errors are present, the center will be displaced both vertically and horizontally. The effect of the pyramidal error is to rotate the line of intersection of the two planes of the equivalent wedge so that it is neither vertical nor horizontal. If the beam is incident first on AB, the return beam reflected from the internal face of AB will be nearly parallel to the one reflected from AB externally, and hence we again get Haidinger fringes due to the interference of these two beams. This arrangement checks the exactness of the 90° angle of the angle C. If the center of the Haidinger fringes is not displaced horizontally, the 90° angle is exact; and, if in addition there

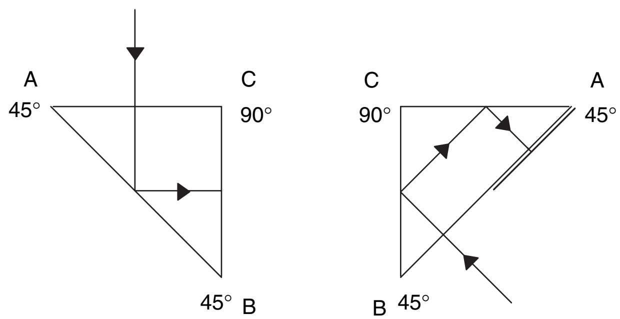

FIGURE 1.38. Schematic of the 45° −90° −45° prism to be equivalent parallel plates of glass.

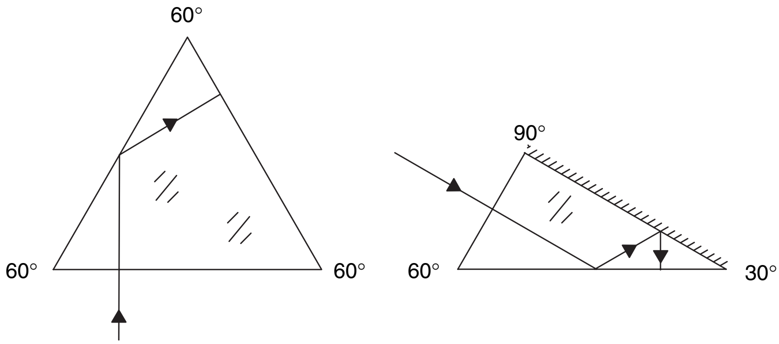

FIGURE 1.39. Schematics of two other prisms to be equivalent parallel plates of glass.

is no vertical displacement, there is no pyramidal error. More details of this method may be found in the paper by Saxena and Yeswanth (1990).

Other examples of prisms that may be treated as equivalent parallel plates are shown in Figure 1.39. Readers may come across other examples depending on particular situations.

The formula given in Eq. (1.27) is applicable in the situations described noting that the displacement has two components, one in the vertical direction and one in the horizontal direction.

1.5. ABSOLUTE TESTING OF FLATS

Until now, we have considered the testing of flats against a "perfect" flat taken as a reference. It is, however, often necessary to make a flat when a good reference flat is not available. In this case, an alternative is to use a liquid flat as mentioned in Section 1.2.2. Another possibility is to make three flats at the same time and test them with several combinations in order to obtain the absolute departure of the three surfaces with respect to an ideal flat.

Let us assume that we have three surfaces that will be tested in many combinations by placing them in pair, one against the other. One of the two glass disks (A) is placed on top of the other by flipping in x by rotation about an axis that is parallel to the y-axis. If the surface deformation is represented by $F_A(x, y)$ as illustrated in Figure 1.40 (a), it is now expressed by

$$[F_A(x, y)]_x = -F_A(-x, y) \tag{1.29}$$

The glass disk at the bottom (B) may be rotated by an angle θ with respect to its original position, as in Figure (1.40)(c). Then, its surface deformation is represented by $[F_B(x, y)]_\theta$ as expressed by

$$[F_B(x, y)]_\theta = F_B(x \cos\theta - y \sin\theta,\ x \sin\theta + y \cos\theta) \tag{1.30}$$

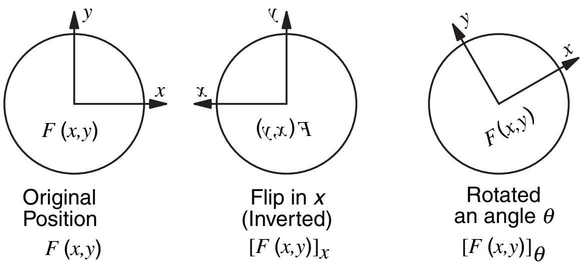

FIGURE 1.40. Three possible orientations for the surfaces whose deviations with respect to an ideal plane are to be determined.

Then, by measuring the fringe pattern we can obtain the value of the difference:

$$G_{BA}(x, y) = [F_B(x, y)]_\theta - [F_A(x, y)]_x \tag{1.31}$$

If, following the treatment by Schulz and Schwider (1976) we take $\theta = 0$ and take the three possible combinations, (see Figure 1.41) we obtain

$$\begin{aligned} G_{BA}(x, y) &= F_B(x, y) + F_A(-x, y) \\ G_{CA}(x, y) &= F_C(x, y) + F_A(-x, y) \\ G_{CB}(x, y) &= F_C(x, y) + F_B(-x, y) \end{aligned} \tag{1.32}$$

This system has more unknowns than equations. Along the y axis, if we make $x = 0$, the system has a simple solution. A solution for all the plane can be obtained only the

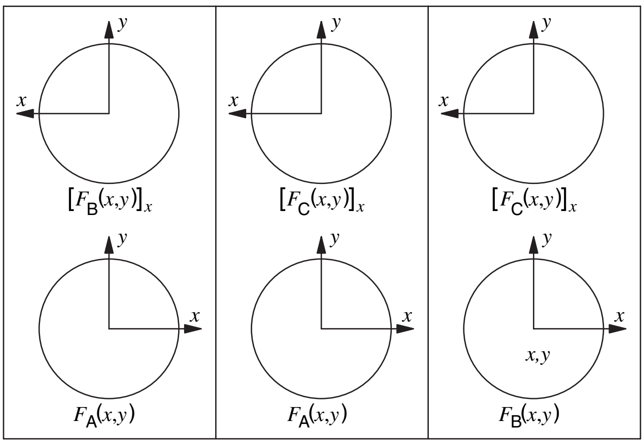

FIGURE 1.41. Three different combinations for the three surfaces to be measured.

if the symmetry about the y axis at least for one surface is assumed, for example for surface B, by taking $F_B(x, y) = F_B(-x, y)$. Then, we may obtain

$$
\begin{aligned}
F_A(x, y) &= \frac{G_{BA}(-x, y) + G_{CA}(-x, y) - G_{CB}(-x, y)}{2}, \\
F_B(x, y) &= \frac{G_{BA}(x, y) - G_{CA}(x, y) + G_{CB}(x, y)}{2}, \\
F_C(x, y) &= \frac{G_{CA}(x, y) - G_{BA}(x, y) - G_{CB}(x, y)}{2}.
\end{aligned} \tag{1.33}
$$

Several other methods had been devised, for example by Truax (1988). A specially interesting method is that of Ai and Wyant (1992) as follows next. Let us assume that the shape of one of the surfaces may be represented by the function $F(x, y)$. Any one-dimensional asymmetrical function can be represented by the sum of one even (symmetrical) function and one odd (antisymmetrical) function. On the contrary, for any asymmetrical function $f(x)$ the following properties hold:

$$
\begin{aligned}
&(1) \quad F_e(x) = f(x) + f(-x) \qquad \text{is even,} \\
&(2) \quad F_o(x) = f(x) - f(-x) \qquad \text{is odd.}
\end{aligned} \tag{1.34}
$$

Generalizing this result to two dimensions

$$
\begin{aligned}
&(1) \quad F_{ee}(x, y) = f(x, y) + f(-x, y) + f(x, -y) + f(-x, -y) \quad \text{is even-even;} \\
&(2) \quad F_{eo}(x, y) = f(x, y) + f(-x, y) - f(x, -y) - f(-x, -y) \quad \text{is even-odd;} \\
&(3) \quad F_{oe}(x, y) = f(x, y) - f(-x, -y) + f(x, y) - f(-x, y) \quad \text{is odd-even;} \\
&(4) \quad F_{oo}(x, y) = f(x, y) - f(-x, y) + f(x, -y) - f(-x, y) \quad \text{is odd-odd.}
\end{aligned} \tag{1.35}
$$

The conclusion is that any two-dimensional asymmetric function $F(x, y)$ can always be decomposed into the sum of four functions, even-even, even-odd, odd-even, and odd-odd as follows:

$$
F(x, y) = F_{ee} + F_{oo} + F_{oe} + F_{eo}, \tag{1.36}
$$

where

$$
\begin{aligned}
F_{ee}(x,\ y) &= (F(x,\ y) + F(-x,\ y) + F(x,\ -y) + F(-x,\ -y))/4, \\
F_{oo}(x,\ y) &= (F(x,\ y) - F(-x,\ y) - F(x,\ -y) + F(-x,\ -y))/4, \\
F_{eo}(x,\ y) &= (F(x,\ y) + F(-x,\ y) - F(x,\ -y) - F(-x,\ -y))/4, \\
F_{oe}(x,\ y) &= (F(x,\ y) - F(-x,\ y) + F(x,\ -y) - F(-x,\ -y))/4.
\end{aligned} \tag{1.37}
$$

Let us now assume that we test two flats with surface shapes $F_A(x, y)$ and $F_B(x, y)$ by placing one over the other. Following Ai and Wyant, eight combinations are selected,

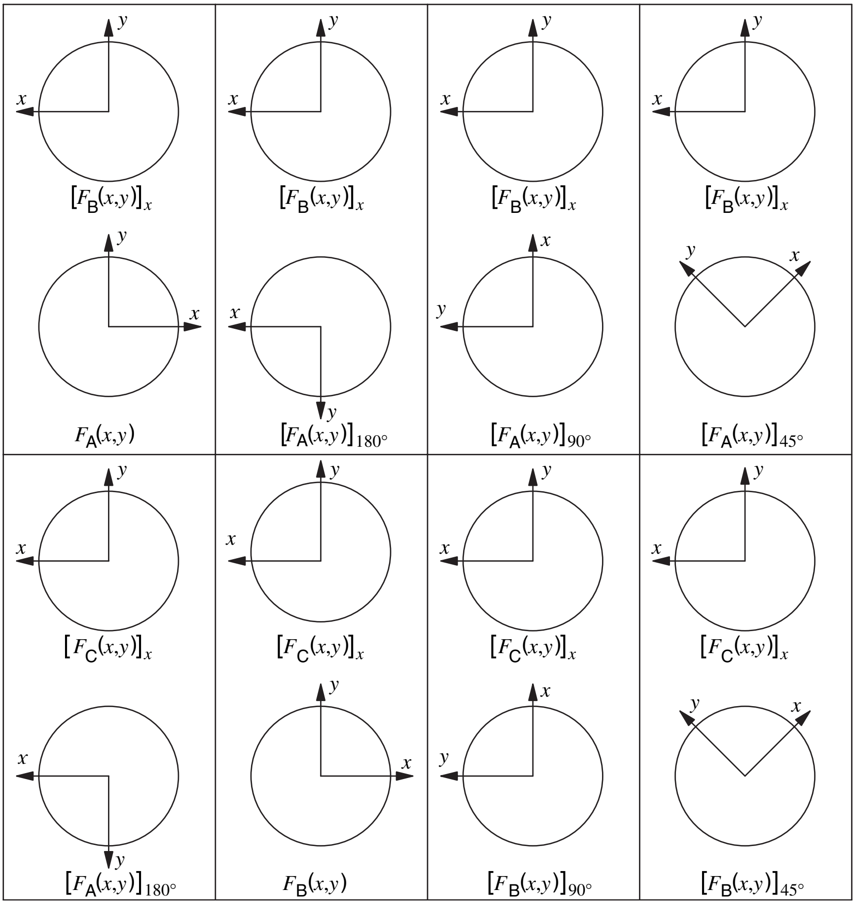

FIGURE 1.42. Eight different combinations for the three surfaces to be measured.

as in Figure 1.42, where the optical path difference producing Newton or Fizeau fringes will be

$$\begin{aligned}
G_1(x,y) &= [F_B(x,y)]_x - F_A(x,y) \\
G_2(x,y) &= [F_B(x,y)]_x - [F_A(x,y)]_{180} \\
G_3(x,y) &= [F_B(x,y)]_x - [F_A(x,y)]_{90} \\
G_4(x,y) &= [F_B(x,y)]_x - [F_A(x,y)]_{45} \\
G_5(x,y) &= [F_C(x,y)]_x - [F_A(x,y)]_{180} \\
G_6(x,y) &= [F_C(x,y)]_x - F_B(x,y) \\
G_7(x,y) &= [F_C(x,y)]_x - [F_B(x,y)]_{90} \\
G_8(x,y) &= [F_C(x,y)]_x - [F_B(x,y)]_{45}
\end{aligned} \tag{1.38}$$

With these expressions, the entire profile of the three planes can be calculated. First, the odd-even, the even-odd, the even-even, and the odd-odd components of the three desired functions $F_A(x, y)$, $F_B(x, y)$, and $F_C(x, y)$ are calculated. The odd-odd component is the most difficult to evaluate, which is obtained using Fourier sine series. Tilt and piston term are not obtained, but this is not a problem since they do not have any practical interest.

Fritz (1983 and 1984) proposed a method using Zernike polynomials to decompose the desired functions into orthogonal functions. Later, Shao et al. (1992) found that by neglecting some high spatial frequencies, the solution can be obtained by using only four combinations.

REFERENCES

Ai C. and J. Wyant, "Effect of Spurious Reflection on a Phase Shift Interferometry," *Appl. Opt.*, **27**, 3039–3045 (1988).

Ai C. and J.C. Wyant, "Absolute Testing of Flats Decomposed to Even and Odd Functions," *Proc. SPIE,* **1776**, 73–83 (1992).

Ai C. and J. Wyant, "Effect of Retroreflection on a Phase-Shifting Interferometer," *Appl. Opt.*, **32**, 3470–3478 (1993).

Burge J. H., "Fizeau Interferometry for Large Convex Surfaces," *Proc. SPIE*, **2536**, 127–138 (1995).

Deck L., D. Stephenson, M. Küchel, and C. Evans, "Advances in Laser Fizeau Inteferometry for Optical Testing," *TOPS*, **76**, 108–111 (2000).

Forman P. F., "A Note on Possible Errors Due to Thickness Variations in Testing Nominally Parallel Plates," *Appl. Opt.*, **3**, 646 (1964).

Forman P. F., "The Zygo Interferometer System," *Proc. SPIE*, **192**, 41 (1979).

Fritz B. S., "Absolute Calibration of an Optical Flat," *Proc. SPIE*, **433**, 123 (1983).

Fritz B. S., "Absolute Calibration of an Optical Flat," *Opt. Eng.*, **23**, 379 (1984).

Grigor'ev V. A., Va. O. Zaborov, and P. P. Ivanov, "Use of a Liquid Mirror for the Calibration of an Interferometer," *Sov. J. Opt. Technol.*, **53**, 613 (1986).

Hariharan P. and W. H. Steel, "Fringe Localization Depth: A Comment," *Appl. Opt.*, **28**, 29 (1989).

Karow H. H., "Interferometric Testing in a Precision Optics Shop: A Review of Testplate Testing," *Proc. SPIE*, **192**, 56 (1979).

Ketelsen D. A. and D. S. Anderson, "Optical Testing With Large Liquid Flats," *Proc. SPIE*, **966**, 365 (1988).

Malacara D. and A. Cornejo, "Testing of Aspherical Surfaces with Newton Fringes," *Appl. Opt.*, **9**, 837 (1970).

Moore R. C. and F. H. Slaymaker, "Direct Measurement of Phase in a SphericalWave Fizeau Interferometer," *Appl. Opt.*, **19**, 2196 (1980).

Murty M. V. R. K., "A Note on the Testing of Large Aperture Plane Parallel Plates of Glass, "*Appl. Opt.*, **2**, 1337 (1963).

Murty M. V. R. K., "Addendum to: A Note on the Testing of Large Aperture Plane Parallel Plates of Glass," *Appl. Opt.*, **3**, 784 (1964a).

Murty M. V. R. K., ‘‘The Use of a Single Plane Parallel Plate as a Lateral Shearing Interferometer with a Visible Gas Laser Source,’’ *Appl. Opt.*, **3**, 531 (1964b).

Murty M. V. R. K. and R. P. Shukla, ‘‘Some Considerations of the Fizeau Interferometer,’’ *Bull. Opt. Soc. India*, **4**, 13 (1970).

Novak E., C, Ai and C. Wyant, ‘‘Errors Caused by Nearly Parallel Optical Elements in a Laser Fizeau Interferometer Utilizing Strictly Coherent Imaging,’’ *Proc. SPIE*, **3134**, 456–460 (1997).

Primak W., ‘‘Optical Flatness Standard,’’ *Opt. Eng.*, **23**, 806 (1984).

Primak W., ‘‘Optical Flatness Standard II: Reduction of Interferograms,’’ *Proc. SPIE*, **954**, 375 (1989a).

Primak W., ‘‘Optical Flatness Standard: Comment,’’ *Opt. Eng.*, **28**, 934 (1989b).

Saxena A. K. and L. Yeswanth, ‘‘Low Cost Method for Subarcsecond Testing of a Right Angle Prism,’’ *Opt. Eng.*, **29**, 1516–1520 (1990).

Schulz G. and J. Schwider, in *Progress in Optics*, vol. **13**, E. Wolf, Ed., North Holland, Amsterdam, 1976, Chap. IV.

Schulz G. and J. Schwider, ‘‘Comments on the Paper ‘‘Optical Flatness Standard,’’ *Opt. Eng.*, **26**, 559 (1987).

Shack R. V. and G. W. Hopkins, ‘‘The Shack Interferometer,’’ *Opt. Eng.*, **18**, 226 (1979).

Simon J. M. and S. A. Comatri, ‘‘Fringe Localization Depth,’’ *Appl. Opt.*, **26**, 5125 (1987).

Smith W. S., ‘‘Versatile Interferometer for Shop Use,’’ *Proc. SPIE*, **192**, 13 (1979).

Taylor W. G. A., ‘‘Spherical Aberration in the Fizeau Interferometer,’’ *J. Sci. Instrum.*, **34**, 399 (1957).

Truax B. E., ‘‘Absolute Interferometric Testing of Spherical Surfaces,’’ *Proc. SPIE*, **966**, 130 (1988).

Vannoni M. and G. Molezini, ‘‘Joint Interferometric Measurement of Planarity and Parallelism,’’ *Opt. Eng.*, **43**, 1215–1220 (2004).

Wasilik H., T. V. Biomquist, and C. S. Willet, ‘‘Measurement of Parallelism of the Surfaces of a Transparent Sample Using Two Beam Nonlocalized Fringes Produced by Laser,’’ *Appl. Opt.*, **10**, 2107 (1971).

Wyant J. C., ‘‘Fringe Localization,’’ *Appl. Opt.*, **17**, 1853 (1978).

Yoder P. R., Jr. and W. W. Hollis, ‘‘Design of a Compact Wide Aperture Fizeau Interferometer,’’ *J. Opt. Soc. Am.*, **47**, 858 (1957).